




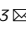




Type VII secretion systems: structure, functions and transport models

Angel Rivera-Calzada¹  , Nikolaos Famelis^{2,3} , Oscar Llorca¹ 
and Sebastian Geibel^{2,3}  

Abstract | Type VII secretion systems (T7SSs) have a key role in the secretion of effector proteins in non-pathogenic mycobacteria and pathogenic mycobacteria such as *Mycobacterium tuberculosis*, the main causative agent of tuberculosis. Tuberculosis-causing mycobacteria, still accounting for 1.4 million deaths annually, rely on paralogous T7SSs to survive in the host and efficiently evade its immune response. Although it is still unknown how effector proteins of T7SSs cross the outer membrane of the diderm mycobacterial cell envelope, recent advances in the structural characterization of these secretion systems have revealed the intricate network of interactions of conserved components in the plasma membrane. This structural information, added to recent advances in the molecular biology and regulation of mycobacterial T7SSs as well as progress in our understanding of their secreted effector proteins, is shedding light on the inner working of the T7SS machinery. In this Review, we highlight the implications of these studies and the derived transport models, which provide new scenarios for targeting the deadly human pathogen *M. tuberculosis*.

Many bacteria rely on highly specialized macromolecular nanomachines embedded in their cell envelopes to inject effector proteins into eukaryotic or prokaryotic cells, or to release them into the extracellular environment¹. These nanomachines were initially described in bacterial pathogens that were able to transfer effector proteins to target cells and modulate cellular functions in the host^{2–4}. The secreted proteins mediate a variety of functions, including scavenging, adhesion, modulation of symbiotic, intraspecific and interspecific interactions, and bacterial fitness¹.

Nine secretion system types have been identified to date (I to IX), with distinct structures and secretion mechanisms^{5,6}. Moreover, a recent study suggests the existence of a type X secretion system⁷. Substrates can be translocated across one, two or three membranes in the case of secretion systems that release substrates into the host cytoplasm. Depending on the architecture of the secretion system, substrates are transferred in a one-step process directly from the bacterial cytosol to its target location or in a two-step mechanism, in which substrates are first transferred to the periplasm, followed by a second transfer step across the outer membrane by specialized nanomachines. Substrates can be translocated across the secretion system in their native conformation, partially folded or unfolded, by energy-dependent transport mechanisms that rely on diverse energy sources, including ATP, entropy gradients of the protein substrates or ion gradients across the bacterial inner membrane⁵.

Several secretion systems can coexist in the same bacterium, and their presence often correlates with pathogenicity, which makes them candidate targets for novel therapeutic approaches⁸. Secretion systems can be organized as gene clusters or operons in genomes or plasmids. The genetic organization often reveals the origin of these nanomachines, and how nature has assigned new functions to ancestral machineries like the type III secretion system, which also constitute the core of flagellar motility machines, or the type VI secretion system, which contains a phage-like injection apparatus^{9,10}.

Structural analysis of these complex nanomachines has proved difficult over the years because they are flexible multiprotein complexes, are difficult to overexpress and they need to be purified from the bacterial cell envelope in native conditions. Advances in cryogenic electron microscopy (cryo-EM) are helping in surpassing these limitations¹¹, and are revealing at unprecedented detail the complexity and molecular mechanisms of these highly specialized macromolecular complexes⁶.

The first type VII secretion system (T7SS) was discovered during study of the pathogen *Mycobacterium tuberculosis*, the main causative agent of tuberculosis. Tuberculosis is the infectious disease that has killed most people throughout history¹², and it is still one of the top ten causes of death worldwide. In 1995, P. Andersen and colleagues identified a novel antigen secreted by *M. tuberculosis* into culture filtrates: the 6-kDa early secretory antigenic target (ESAT-6)². Analyses of the *M. tuberculosis* genome showed that ESAT-6 and its

¹Structural Biology Programme, Spanish National Cancer Research Centre (CNIO), Madrid, Spain.

²Institute for Molecular Infection Biology, Julius–Maximilian University of Würzburg, Würzburg, Germany.

³Rudolf Virchow Center for Integrative and Translational Biomedicine, Julius–Maximilian University of Würzburg, Würzburg, Germany.

✉e-mail: ariverac@cnio.es; sebastian.geibel@uni-wuerzburg.de

<https://doi.org/10.1038/s41579-021-00560-5>

co-secreted partner 10-kDa culture filtrate protein (CFP-10)¹³, later renamed *EsxA* and *EsxB*, respectively, lack canonical cleavable signal peptides at their amino termini (N termini) characteristic of the Sec or Tat secretion pathways¹⁴. The *esxA*–*esxB* operon and those of homologous genes were found to localize within five gene clusters, each harbouring a membrane-associated ATPase and other putative components of secretion systems, indicating the existence of five distinct paralogous secretion systems^{14–17}.

Subtractive hybridization studies revealed that the tuberculosis vaccine strain *Mycobacterium bovis* bacillus Calmette–Guérin (BCG) lacks the *esxA* and *esxB* genes owing to the loss of the genetic region of difference 1 (RD1)^{18,19}, which was later shown to be mainly responsible for its attenuation^{20–22}.

It was subsequently demonstrated that the genes surrounding *esxA* and *esxB* encode an alternative secretion system, which has been given different names: ESAT-6, ESX (ESAT-6 secretion)²³, SNM (secretion in mycobacteria)²⁴ and Wss (WXG100 secretion system)²⁵. Later, the more generic term ‘type VII secretion system’ (T7SS) was coined, referring to all homologous ESX systems in high-G+C Actinobacteria²⁶.

The five paralogous *esx* loci (*esx-1* to *esx-5*) are widespread among fast-growing and slow-growing mycobacteria, whereas the numbers of encoded ESX systems differ between mycobacterial strains²⁷. In addition, plasmid-encoded ESX secretion systems were discovered in fast-growing mycobacteria^{28,29}.

Tuberculosis-causing mycobacteria encode all five *esx* loci, whereas pathogens such as *Mycobacterium leprae* (*esx-1* to *esx-3* and *esx-5*) and *Mycobacterium abscessus* (*esx-3* and *esx-4*) as well as the non-pathogenic *Mycobacterium smegmatis* (*esx-1* to *esx-4*) do not encode all *esx* loci (FIG. 1a).

Conserved genes corresponding to members of the WXG100 protein family (BOX 1) and a membrane-anchored ATPase of the FtsK–SpoIIIE protein family have been identified in low-G+C Firmicutes, leading to the discovery of a new secretion system in the human opportunistic pathogen *Staphylococcus aureus*, which was initially termed the ‘ESAT-6 like secretion system’ (Ess). Owing to the limited genetic conservation between the T7SSs in Actinobacteria and Firmicutes, they were classified as T7SS and T7SSb, respectively²⁶. The aforementioned signature genes were also found in several Gram-negative phyla, including Cyanobacteria and Proteobacteria (for example, *Helicobacter pylori*), but it is unclear whether they represent active secretion systems^{30,31}.

Protein transport across the prototypical ESX secretion machines is powered by one or more substrate-specific ATPases. EccC is the membrane-anchored FtsK–SpoIIIE family ATPase, powering substrate secretion and also acting as the coupling protein, binding substrates before translocation. EccC and the three conserved membrane proteins EccB, EccD and EccE form the stable core of the secretion machine in the inner membrane of the mycobacterial cell envelope whereas MycP, a membrane-anchored protease, is not tightly associated with the core complex^{32–37} (FIG. 1b).

The cytosolic ATPase EccA is required for secretion of a specific subset of substrates and may be recruited to the ESX secretion machine upon substrate binding^{38–40}. Roles of EccA as an instigator of secretion or as an ATP-dependent dissociase for chaperone–substrate complexes have been proposed⁴¹. Recent progress has revealed the molecular organization of ESX-3 and ESX-5 secretion complexes at atomic resolution^{37,42–44}. These structures suggest plausible mechanisms for secretion and are discussed in the sections entitled ‘T7SS architecture’ and ‘Transport models’.

Interestingly, current structural knowledge indicates that the T7SS core complex does not reach the outer mycomembrane. *M. tuberculosis* together with other species in the order Corynebacteriales exhibits a complex cell wall featuring an inner mycomembrane and a unique outer mycomembrane 7–8 nm in thickness in mycobacteria^{45,46}. The inner leaflet of the mycomembrane consists mostly of long-chain mycolic acids (C₆₀–C₉₀), acting as a potent hydrophobic barrier, and is covalently bound to an arabinogalactan layer that anchors the mycomembrane to the peptidoglycan layer⁴⁷. The outer leaflet of the mycomembrane consists of lipids not covalently bound to the cell, proteins and lipopolysaccharides, and is surrounded by a weakly attached capsule, which consists mainly of exopolysaccharides, proteins and a small amount of lipids⁴⁸. According to the mycobacterial diderm cell envelope structure, additional progress is needed to clarify how T7SS substrates are transported across the periplasm and the outer mycomembrane (see the section entitled ‘Transport across the outer mycobacterial membrane’).

The actual secretion process is poorly understood, but common properties described in BOX 1 are shared among T7SS substrates, suggesting the existence of a conserved secretion mechanism for the diverse T7SSs. T7SS substrates carry signal sequences required for transport, and typically form dimers that share a characteristic

Arabinogalactan layer

An essential constituent of the mycobacterial cell wall. Peptidoglycan is covalently attached to the heteropolysaccharide arabinogalactan, which is in turn linked to the mycolic acid layer.

Capsule

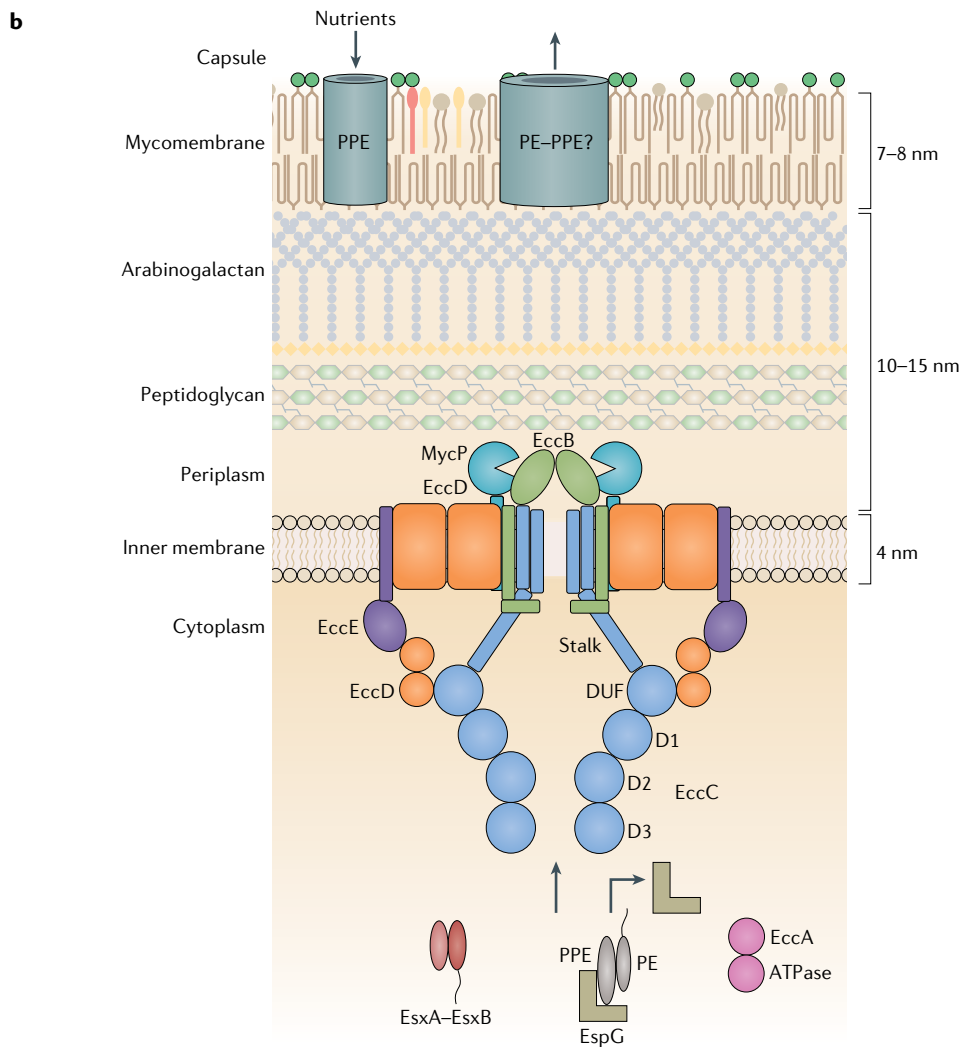
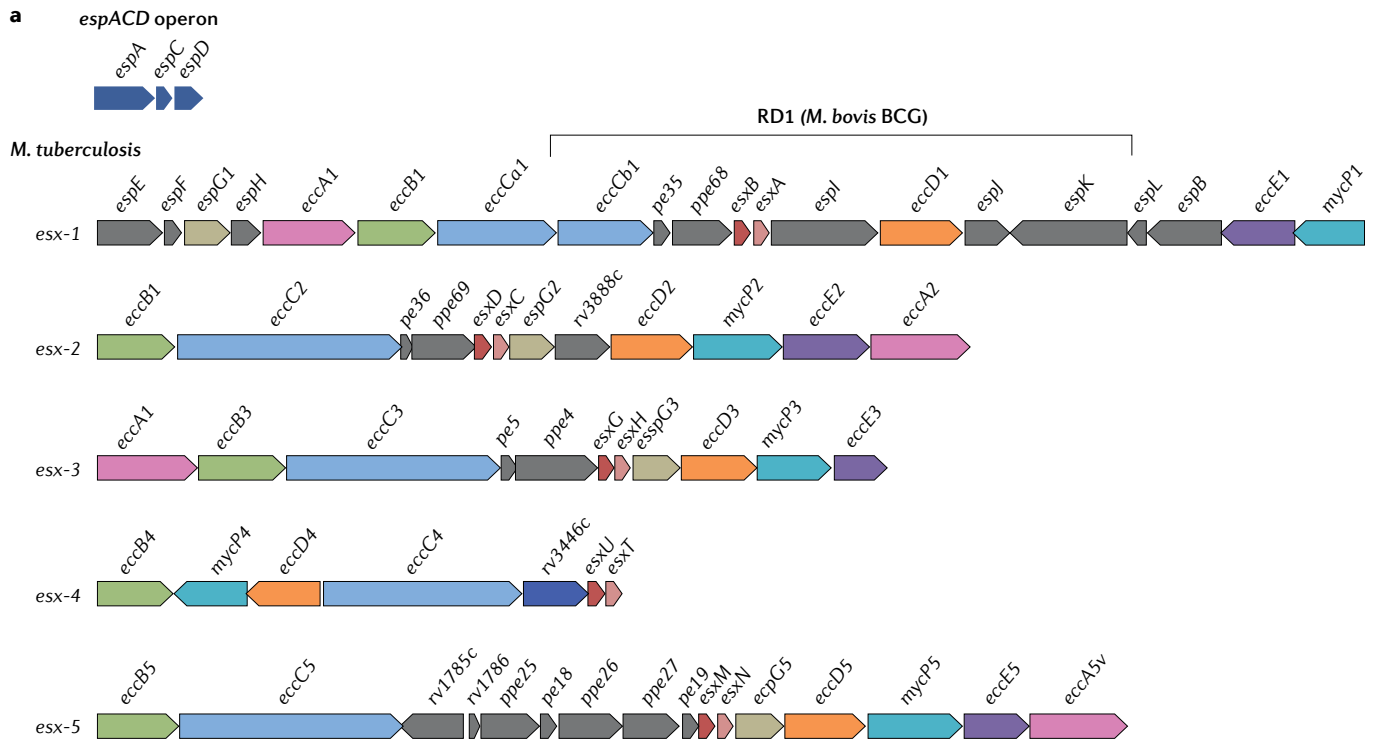
The mycobacterial capsule is the outermost layer of the bacterial cell and consists mainly of a glycogen-like α-glucan with lower amounts of arabinomannan and mannan, proteins and lipids. This layer mediates key interactions with host cells during initial stages of infection and favours bacterial survival.

Diderm

A term to describe the presence of an inner membrane and an outer membrane in the cell envelope such as in Gram-negative bacteria and mycobacteria.

Fig. 1 | Genetic and functional organization of mycobacterial type VII secretion systems.

a | Gene clusters of the five ESX secretion systems in *Mycobacterium tuberculosis*. The region of difference 1 (RD1) is a genetic deletion found in the vaccine strain *Mycobacterium bovis* bacillus Calmette–Guérin (BCG) that is primarily responsible for its attenuation. The *espACD* operon is located upstream of the *esx-1* gene cluster and the expressed substrates are transported through ESX-1. **b** | Functional organization of type VII secretion systems. The conserved membrane components EccB, EccC, EccD, EccE and MycP assemble a secretion machine in the plasma membrane of the mycobacterial cell envelope. The intracellular chaperone EspG prevents aggregation of substrates belonging to the PE–PPE protein family and dissociates before secretion. The cytoplasmic ATPase EccA is required for the secretion of a subset of proteins and has been hypothesized to provide the energy for dissociating EspG from PE–PPE proteins or for instigating secretion of Esx substrates. Some PPE proteins of the PE–PPE protein family mediate the uptake of nutrients. Members of the PE–PPE protein family are therefore potential candidates to form the substrate secretion pore. DUF, domain of unknown function.



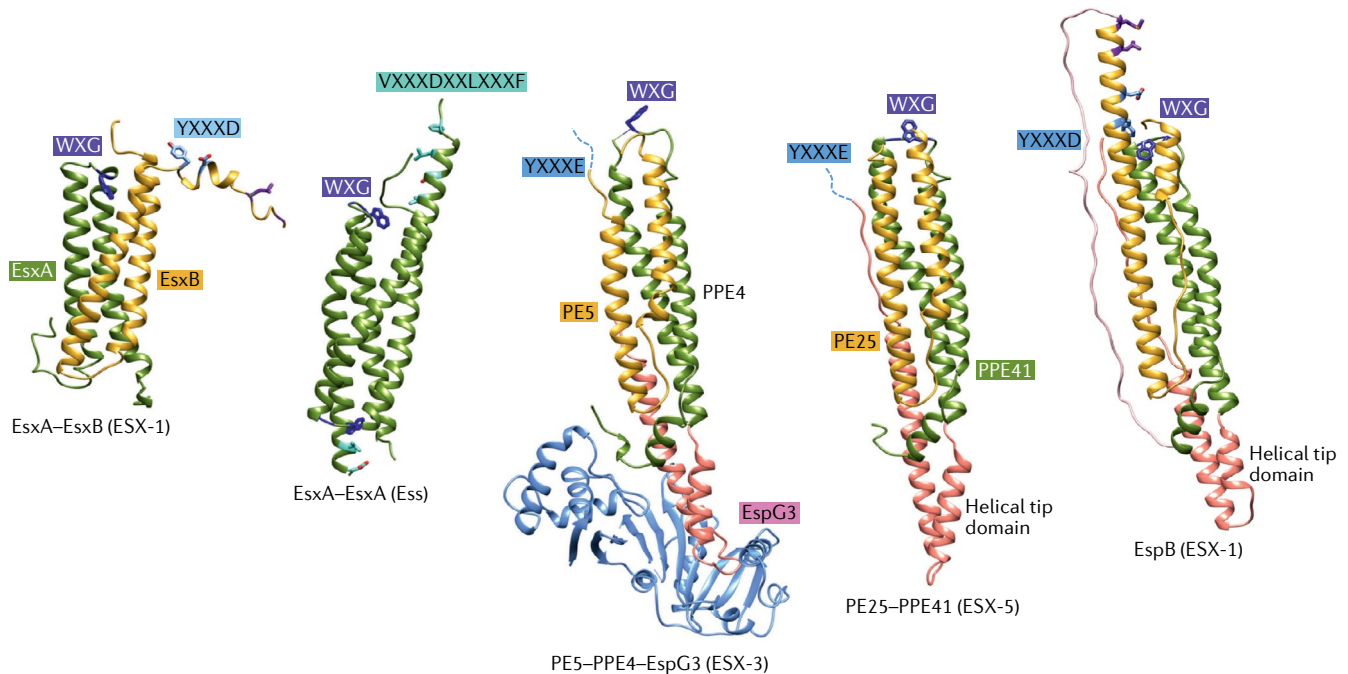
Box 1 | Secreted effector proteins of mycobacterial T7SSs and T7SSb

Type VII secretion system (T7SS) substrates are defined by a conserved YXXXD/E motif or a WXG motif¹⁷⁹. The two motifs are required to form a bipartite secretion signal in spatial proximity for transport. Native substrates lacking either of the two signatures or not having them in proximity are translocated as part of a heterodimeric complex with proteins that contain such motifs. In T7SSb, the YXXXD/E motif is present in the form of HXXXD/EXXhXXXH, in which 'H' and 'h' correspond to highly conserved or less conserved hydrophobic residues¹⁸⁰, respectively, and with the WXG motif forms the bipartite secretion signal¹⁸¹. T7SS substrates are characterized by a helix–turn–helix structure, in which the WXG motif is present between the two α -helices. Homodimerization or heterodimerization results in the typical four-helix bundle structure that has been observed for all substrate proteins so far⁴⁹ and is ~22 Å in diameter, suggestive of the maximal diameter of the transport pore.

Mycobacterial T7SS substrates have traditionally been classified into three different protein families: Esp (ESX-1 secretion-associated proteins), Esx and PE–PPE (Pro–Glu (PE) and Pro–Pro–Glu (PPE)). Esp substrates are secreted through ESX-1. The Esp family contains heterodimers such as EspA–EspC as well as the monomeric substrate EspB, which exhibits the four-helix bundle fold in a single protein^{133,182}. Esx substrates belong to the WXG100 protein family, which are typically ~100 amino acids in length¹⁸³. The best-studied representatives of this class are EsxA and EsxB from *Mycobacterium tuberculosis*. The NMR structure of EsxA–EsxB shows the prototypical four-helix bundle structure in which EsxB carries a WXG motif, a YXXXD motif and a short carboxy-terminal (C-terminal) peptide without apparent sequence conservation⁴⁹. The EccC ATPase recognizes hydrophobic residues in this peptide, which is crucial for secretion^{90,93,184}. EsxA contains the WXG motif, which forms the bipartite

secretion signal together with the YXXXD motif of EsxB. PE and PPE substrates consist of heterodimers formed by the PE protein and its cognate PPE partner¹⁸⁵. Their conserved amino-terminal (N-terminal) domains carry a PE motif and a PPE motif, respectively, and show the characteristic helix–turn–helix motifs and form a four-helix bundle structure upon dimerization. PE proteins comprise an N-terminal domain of ~100 amino acids and carry the YXXXD/E secretion signal at the C terminus. PPE proteins comprise an N-terminal domain of ~180 amino acids and bind to cognate chaperones, including EspG, through a conserved hydrophobic patch in the extended helical tip^{127,186}. PE and PPE proteins are extremely variable in length owing to their diverse C-terminal domains, which allow further classification into different subfamilies^{185,187}.

In the figure, representative structures of the three different T7SS substrate classes are shown. WXG100 substrates: EsxA–EsxB (ESX-1) from *Mycobacterium bovis* (Protein Data Bank (PDB) ID 1WA8) and EsxA–EsxA (Ess/T7SSb) from *Staphylococcus aureus* (PDB ID 2VS0). PE–PPE substrates bound by cytosolic chaperones: hybrid structure of PE5–PPE4 from *M. tuberculosis* bound to the chaperone EspG from *Mycobacterium marinum* (ESX-3; PDB ID 6UJ) and PE25–PPE41 (ESX-5) from *M. tuberculosis* determined in the absence of the chaperone EspG (PDB ID 4W4K). Esp substrates: monomeric EspB (ESX-1) from *M. tuberculosis* (PDB ID 4XY3). The bipartite T7SS secretion signal consists of the WXG motif (blue) and either a YXXXD/E motif (light blue) or a similar HXXXD/EXXhXXXH motif (turquoise). Additional hydrophobic residues (purple) found at the EsxB C terminus are crucial for interaction with EccC motor ATPase and secretion, and are also present in other substrates (for example, EspB).



helix–turn–helix structure⁴⁹. In the case of *M. tuberculosis*, substrates of the T7SS have a key role as virulence factors allowing pathogenic mycobacteria to adapt and survive in the different environments encountered at multiple stages of infection. Therefore, T7SS expression and activity have to be tightly regulated, topics that we introduce in the following section. In addition, T7SS substrates also have key roles in bacterial fitness and survival, including DNA transfer and bacterial competition,

and these roles together with the contribution of tuberculosis substrates to the infectious process are outlined in the section entitled ‘Functions of effector proteins’.

In this Review, we provide an overview of different aspects of the T7SSs taking into account the key structural and functional information provided by the ESX-3 structure from *M. smegmatis*^{37,44} and the preliminary hexameric structures of ESX-5 from *M. tuberculosis* and *Mycobacterium xenopi*^{42,43}.

T7SS transcriptional regulation

In *M. tuberculosis* ESX-1, ESX-3 and ESX-5 are required for full virulence and viability. ESX-5, the most recently evolved ESX system, is involved in nutrient uptake and is essential for growth⁵⁰, is responsible for the secretion of immunomodulatory effector proteins⁵¹ and is exclusive to slow-growing species, which include most pathogenic species such as *M. tuberculosis*, *M. leprae* and *Mycobacterium marinum*⁵². ESX-3 is involved in metal ion acquisition in response to iron-limiting and zinc-limiting conditions and is essential for growth under these conditions^{53–55}, and has additional functions in interfering with the cellular immune system^{56–58}. ESX-1 is crucial for intracellular survival and has key roles in phagosomal rupture as well as host cell lysis enabling translocation into the cytosol and release of *M. tuberculosis* into the extracellular environment^{59–62}.

ESX-4 is considered the ancestral ESX secretion system from which ESX systems might have evolved¹⁵ and is essential for intracellular growth of *M. abscessus* in human phagocytes^{63,64}. *esx-4* loci contain a smaller number of genes when compared with other *esx* loci. Interestingly, *esx-4* loci lack the conserved *espG*, *eccA* and *eccE* (with exception of *M. abscessus*) as well as the *pe-ppe* (Pro-Glu (PE) and Pro-Pro-Glu (PPE)) substrate family genes (BOX 1; FIG. 1a), which might have implications for function. In non-pathogenic *M. smegmatis*, ESX-1 and ESX-4 mediate a special form of interbacterial DNA transfer⁶⁵. The different ESX systems have different roles in bacterial fitness and pathogenicity, and therefore their expression and activity have to be specifically regulated.

The *esx-1* locus is subjected to a multilayered transcriptional regulation^{66,67}. Changes in the environmental conditions are sensed using two-component signal transduction systems (TCSs). These consist of a sensor kinase located in the cytoplasmic membrane that, upon specific stimuli, autophosphorylates and subsequently phosphorylates the cognate response regulator, which becomes active as a transcription factor⁶⁸. In the TCS PhoPR, the sensor kinase PhoR detects environmental changes following phagocytosis of *M. tuberculosis*, such as the acidic pH in the phagosome (reviewed in REF.⁶⁹), and the response regulator PhoP upregulates the *espACD* operon upstream of the *esx-1* locus^{70,71} required for secretion of ESX-1 substrates^{72,73} and promotion of the mycobacterial escape from the phagosome^{59–61}. A second TCS, MprAB, regulates the *espACD* operon in response to cell envelope stress⁷⁴. Additional regulatory factors of the *espACD* operon include EspR, CRP and Lsr2 (REFS^{75–78}). The transcriptional regulation of the *espACD* operon indirectly affects the secretion of proteins encoded in the ESX-1 gene cluster because the secretion of Esp and ESX-1 proteins is mutually dependent^{72,73}. It is noteworthy that regulatory sequences of EspR, PhoP and MprA lie in the *espACD* promoter region^{71,74,78}, which overlaps with the region of difference 8 (RD8), explaining why ESX-1 secretion is deregulated in some lineages of tuberculosis-causing mycobacteria lacking RD8 (REFS^{79,80}).

A second layer of regulation is a negative-feedback autoregulatory mechanism that adjusts ESX-1 substrate

levels to the presence or absence of the ESX-1 membrane complex^{66,81}. This regulation prevents substrate accumulation in the cytoplasm when the ESX-1 membrane complex is not secretion competent and could be beneficial if substrates exhibit a certain degree of toxicity. The presence of the ESX-1 secretion complex in the membrane induces the expression of the transcription factor WhiB6, which in turn induces the expression of ESX-1 substrates. If the ESX-1 secretion complex is absent from the membrane, there is no WhiB6, and ESX-1 substrate expression is reduced^{66,81}. Additional transcription factors could contribute to this process^{67,82}.

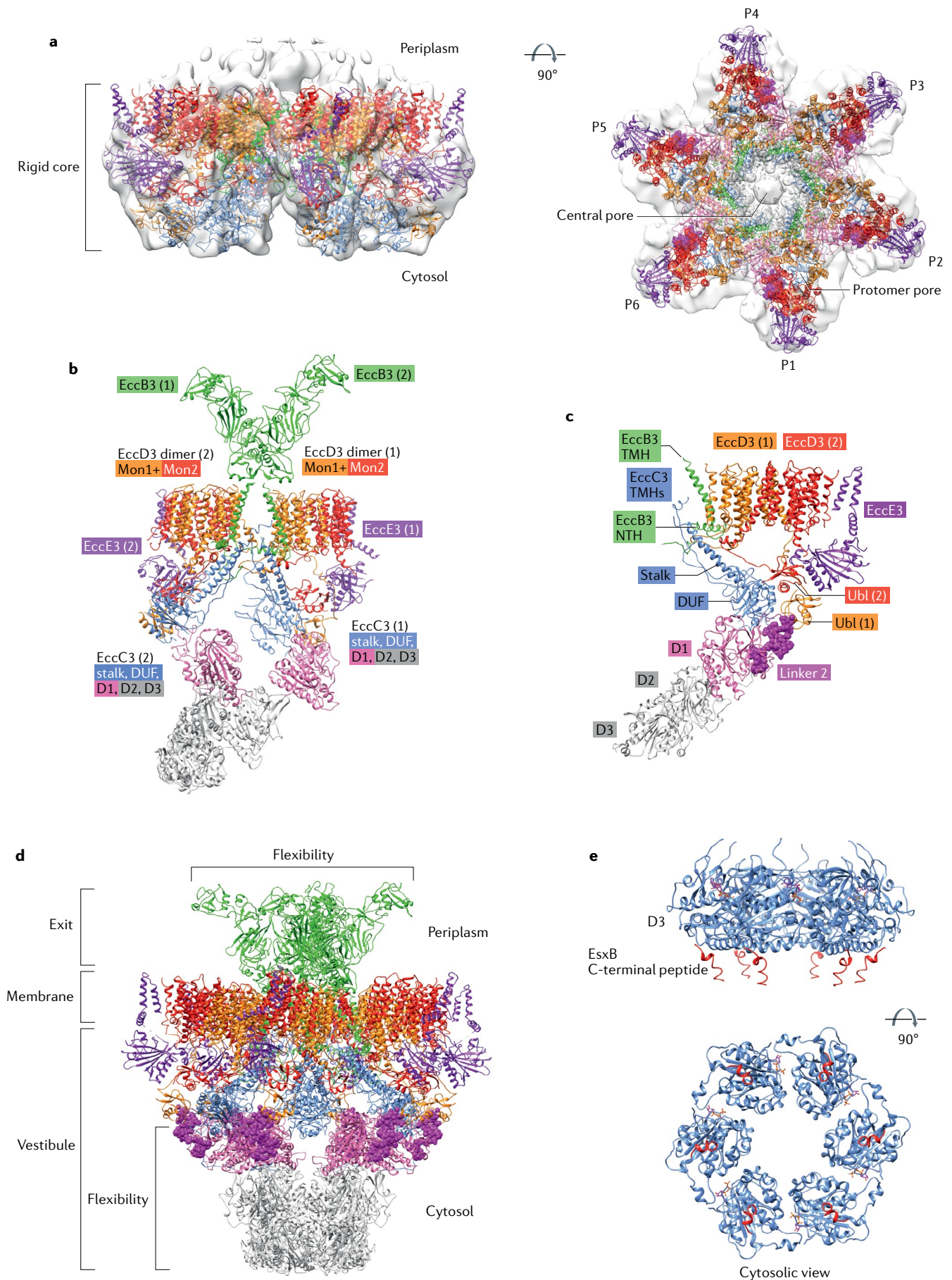
The *esx-3* locus is expressed in response to iron-limiting and zinc-limiting conditions in *M. tuberculosis*, whereas its regulation is independent of zinc in *M. smegmatis*^{83–85}. In *M. tuberculosis*, *esx-3* locus transcription, together with that of genes involved in iron uptake, is negatively regulated by iron-dependent IdeR, a global regulator of iron homeostasis, and in addition by the zinc-dependent Zur repressor^{54,85}. One study suggests that *esx-5* locus transcription is upregulated by the Pst/SenX3–RegX3 system in response to phosphate starvation, in line with the role of ESX-5 in nutrient uptake^{50,86}.

T7SS architecture

The negative-stain electron microscopy structure of the ESX-5 membrane-embedded core complex from *M. xenopi* (EccB–EccC–EccD–EccE) revealed six repeating protomers forming a 5-nm central pore, which is sufficiently wide to allow passage of substrate dimers in their folded state⁸⁷ (FIG. 2a). The ESX-5 hexameric complex has dimensions of 28 nm × 16 nm, and it localizes to the inner mycobacterial membrane. Flexible parts were averaged out owing to the symmetry imposed during data processing and are therefore not visible. However, single particles of the ESX-5 core complex showed that strings of the coupling protein protrude from the stable core, which led to the proposal of a tentacle-like configuration of EccC.

The cryo-EM structure of ESX-3 from *M. smegmatis* resolved the architecture of the membrane core complex in its dimeric state, consisting of two identical protomers, each comprising EccB, EccC, EccD and EccE in a 1:1:2:1 stoichiometry^{37,44} (FIG. 2b). The two ESX-3 protomers are connected by EccB, which dimerizes into a fork-like structure in the periplasm. Four of the five periplasmic domains in EccB show a putative peptidoglycan binding fold, suggesting that it can potentially anchor the secretion machine in the peptidoglycan layer^{88,89}. The unstructured N terminus of one EccB in the dimer forms an intricate network of interactions with both protomers in the cytosol. The N terminus of the second EccB remains free to interact with the next protomer supporting the oligomerization of dimers into hexamers.

At the centre of each protomer, two EccDs dimerize to provide the central scaffold for EccB, EccC and EccE (FIG. 2c). EccD membrane domains form an antiparallel dimer and enclose a large hydrophobic cavity that has been proposed as a possible route for substrate passage, while EccD ubiquitin-like domains anchor the cytosolic EccC and EccE domains^{37,44,88}. EccE contains



◀ Fig. 2 | **Structural model of the membrane-embedded type VII secretion system core complex.** **a** | The negative-stain electron microscopy map of the ESX-5 complex from *Mycobacterium xenopi* at 13-Å resolution (light grey; Electron Microscopy Data Bank (EMDB) entry EMD-3596) reveals the hexameric organization of a type VII secretion system (T7SS) and a central pore. Three ESX-3 dimers obtained by cryogenic electron microscopy (EMDB entry EMD-10186, Protein Data Bank (PDB) ID 6SGW) fit into the ESX-5 map and reveal six additional smaller pores in the protomers. **b** | The cryogenic electron microscopy structure of the ESX-3 dimer reveals the architecture of the T7SS core complex at 3.7-Å resolution and shows additional flexible cytosolic and periplasmic proteins. A fork-like structure formed by dimeric EccB (green) is crucial to hold the two protomers together. The unresolved flexible elements are the EccC domains D2 and D3 (grey). **c** | The EccD dimer (orange and red) acts as central scaffold of the protomer. A small stretch of linker 2 connecting domains D1 and D2 in EccC that is critical for specificity and secretion of PE–PPE substrates is shown as pink spheres. **d** | Structural model of the complete T7SS core complex based on ESX-3 (PDB IDs 6SGW and 6SGY) and the ESX-5 negative-stain map (EMDB entry EMD-3596). **e** | Hexameric model of the D3 ATPase ring bound to signal peptides from EsxB (EsxB–Pep). The model is based on the crystal structure of the EccC D3 monomeric domain (ESX-1) from *Mycobacterium tuberculosis* (PDB ID 6J19)^{93,94} superimposed onto the FtsK motor hexameric domain (PDB ID 2IUU)¹⁷⁸. C-terminal, carboxy-terminal; DUF, domain of unknown function; Mon, monomer; NTH, amino-terminal α -helix; TMH, transmembrane α -helix; Ubl, ubiquitin-like domain.

two transmembrane α -helices (TMHs), and its cytosolic domain has structural homology to glycosyltransferases but lacks key catalytic residues to perform their function. EccE is required for protomer stability and is essential for secretion³⁷. Interestingly, EccE is missing in most ESX-4 systems, except in *M. abscessus*⁶⁴. This raises the question of whether ESX-4 core complexes differ in their protomer architecture. Several conformations of EccC were observed, which could be related to the dynamics required as a motor of substrate transport. EccC contains two TMHs followed by a stalk domain connecting a flexible array of four ATPase domains (DUF (domain of unknown function), D1, D2 and D3) to the membrane. The crystal structure of an EccC cytosolic segment from *Thermomonospora curvata* showed that D1–D3 are connected through linker–pocket interactions that resemble the interaction of the substrate’s signal peptide with the D3 pocket, suggesting that D1 and D2 could also participate in substrate binding upon linker displacement⁹⁰.

Higher molecular weight species of ESX-3 were observed in mycobacterial lysates but could not be extracted stably, suggesting that the dimer is a stable building block³⁷. Structural superimposition of the ESX-3 dimer with the negative-stain ESX-5 hexamer structure indicates that T7SSs are trimers of dimers and provided the first molecular model of a T7SS^{37,87} (FIG. 2a,d). In this hexameric model, three EccB forks flexibly attached to the membrane region assemble into a tight triangular structure that blocks the exit of the membrane pore in the periplasm, while six EccC ATPases form a vestibule-like structure in the cytoplasm comprising 24 ATPase domains (DUF and D1–D3) (FIG. 2d).

A recent preprint presents the cryo-EM structure of the complete inner membrane ESX-5 assembly from *M. tuberculosis*, including all membrane components (EccB–EccE and MycP)⁴³. This structure confirms the stoichiometry of the ESX-3 protomers (1:1:2:1 EccB–EccC–EccD–EccE) and the proposed structural organization of T7SSs as trimers of dimers, and in addition reveals

a central periplasmic dome-like compartment above the central membrane pore consisting of three fork-like EccB dimers stabilized by three MycP molecules.

A second preprint presenting the cryo-EM structure of the ESX-5 core complex from *M. xenopi* (EccB–EccE without MycP)⁴² shows a different organization as a symmetrical hexamer, and in the absence of MycP a different elongated keel-like arrangement of EccB with pseudo C2 symmetry, which is strikingly different from the periplasmic dome-like structure formed by EccB and MycP in ESX-5 from *M. tuberculosis*. In both ESX-5 structures the interior of the central membrane pore is occluded by the bundles of EccC TMHs, which differ from each other in their structural arrangement with respect to the surrounding EccB TMHs.

In their hexameric state T7SS core complexes comprise 24 ATPase domains (DUF and D1–D3). In ESX-5 from *M. tuberculosis*, ATPase domains D1, D2 and D3 of EccC adopt two characteristic conformations: extended and contracted. In the extended conformation, D1–D3 runs parallel to the membrane, emerging radially from the membrane complex. The contracted conformation correlates with the ESX-3 vestibule structure, in which D1–D3 from all six protomers converges in the cytoplasm (FIG. 2d). Transport through the central pore would require the rearrangement of the central TMH bundle observed in both ESX-5 structures. How this rearrangement would occur is currently unknown but could be induced by the rearrangement of the ATPase domains from EccC. As the open state of the membrane pore is unknown, it remains elusive whether substrates are transported in their folded or unfolded state across the T7SS membrane pore. However, the current model for the cytoplasmic ATPase barrel suggests the transport of folded substrates (see the next paragraph).

EccC belongs to the FtsK–HerA and AAA+ ATPase superfamilies⁹¹, which are versatile motor proteins and work as hexameric rings in which two adjacent subunits form the active site⁹². In the active T7SS, EccC ATPase domains could therefore form a four-tier barrel structure with an internal diameter of 25–30 Å (REFS^{93,94}). As the diameter of all known substrate structures is ~22 Å, this model would be compatible with the transport of substrates in their folded state (BOX 1).

ATPase domains D1, D2 and D3 perform different functions. ATPase activity of D1 is crucial for secretion. Linker 2, connecting D2 to D1, inhibits ATPase activity of D1, and therefore this should be uncoupled for activation⁹⁰ (FIG. 2c,d). By contrast, the function of D2 and D3 is to modulate D1 ATPase activity rather than to contribute to the overall ATPase activity of EccC. The carboxy-terminal (C-terminal) D3 domain forms the cytosolic entry to the ATPase barrel and has additional functions in substrate targeting⁹⁰ (FIG. 2e). DUF has been unnoticed as an ATPase domain owing to the lack of canonical Walker A and Walker B motifs. Recent work indicated that DUF is a functional ATPase with an essential function in secretion³⁷. DUF is connected to the EccC stalk domain, which makes electrostatic interactions with the cytosolic α -helix and the TMH of EccB. These interactions suggest that conformational changes

in the EccC stalk domain triggered by DUF ATPase activity or DUF displacement during substrate transport could be coupled to the aperture of the periplasmic exit pore formed by EccB and MycP^{37,43}.

In addition to providing energy to the system, EccC acts as a coupling protein, targeting substrates in the cytosol before translocation. Substrate interaction is thought to stabilize the vestibule and induce the transformation into a hexameric barrel, turning the ESX membrane complex into a secretion-competent machine, which creates the mechanical motion for substrate transport by cycling through conformational states of ATP binding and hydrolysis³⁷.

Structural and mechanistic relationships between T7SSs and T7SSb. T7SSb is predominantly found in low-G+C Firmicutes and is best characterized in *S. aureus*, *Streptococcus intermedius* and *Bacillus subtilis*, and has been associated with bacterial infection (for example, abscess formation in *S. aureus* infection), the development of colon tumours and intoxication of bacterial competitors^{31,95,96}.

Unlike in derm mycobacteria, secreted proteins pass a monoderm cell wall in Firmicutes, indicating a different overall architecture of T7SSs and T7SSb. Both systems share substrates of the WXG100 protein superfamily and a motor ATPase of the FtsK–SpoIIIE ATPase family, suggesting a conserved transport mechanism across the cytoplasmic membrane for these substrates. A distinguishing feature of T7SSb compared with T7SSs is the presence of antibacterial toxins of the polymorphic (F/L)XG family^{97–100}.

The T7SSb core machinery comprises four membrane proteins, EssA, EssB, EssC and EsaA, constituting the core secretion machine in the bacterial cell envelope, one cytosolic component, EsaB, and one secreted substrate, EsxA (to use the T7SSb nomenclature from *S. aureus*)^{101–104} (FIG. 3a,b). Although the core machinery is conserved, there is high variability in the number and composition of secreted effector proteins across different species and strains^{105,106}.

Structural information on the components EssB, EssC and EsaA indicates a distinct T7SSb architecture with limited similarity to the mycobacterial T7SS^{98,107–109} (FIG. 3c). EsaB interacts with the T7SSb membrane complex and shows a ubiquitin-like fold like the EccD cytosolic domain of T7SS, pointing to a possible role as a scaffold protein^{37,44,110} (FIG. 3d).

EssC features two N-terminal FHA domains (FIG. 3e) and shares a conserved C-terminal architecture with T7SS motor proteins comprising two TMHs, a stalk domain and a linear array of four potential P-loop ATPase domains (DUF, D1, D2 and D3)^{94,111,112}. The nucleotide-binding motifs of DUF are degenerate, and its function remains elusive. Unlike its T7SS counterpart, EssC forms hexamers in the absence of other core components and substrates^{112,113}, suggesting that substrate-induced oligomerization is not a requirement for T7SSb activation. The conservation of amino acids mediating the inhibitory interaction between the D1 pocket and linker 2 suggests a mechanism for inhibition and allosteric activation of D1 similar to that in T7SSs.

The T7SSb secretion machine uses two substrate recruitment sites. In *S. aureus*, substrates EsxB and EsxC are targeted to a segment encompassing D2 and D3 that forms the entry to the ATPase barrel¹¹². Analogously to T7SSs, a hydrophobic pocket on D3 is crucial for secretion and probably interacts with the signal peptide of the substrate¹¹² (FIG. 3f). By contrast, the secreted core component EsxA does not interact with the D2–D3 segment in *S. aureus*¹¹⁴. Preliminary research in *B. subtilis* showed that EsxA and the antibacterial toxin YxiD interact with the EssB pseudokinase domain, which is connected via two FHA domains to the motor ATPase⁹⁸. This suggests a function of the FHA domains in coupling substrate targeting and transport. EssB and the FHA domains as well as EsaA are unique structural features of T7SSb.

EsaA is the only cell envelope-spanning component of the system¹¹⁵. A recent preprint showed that the EsaA tip domain from *S. aureus* has similarity to bacterial lectins, suggesting a function in cell adhesion during host infection or targeting of prey bacteria¹¹⁶. The same study revealed that a proteolysis-resistant extracellular fragment of EsaA has bactericidal activity and lyses phospholipid membranes *in vitro*¹¹⁶, and therefore could facilitate the delivery of effector proteins into prokaryotic or eukaryotic target cells analogously to secretion systems of types I, II, III and VI.

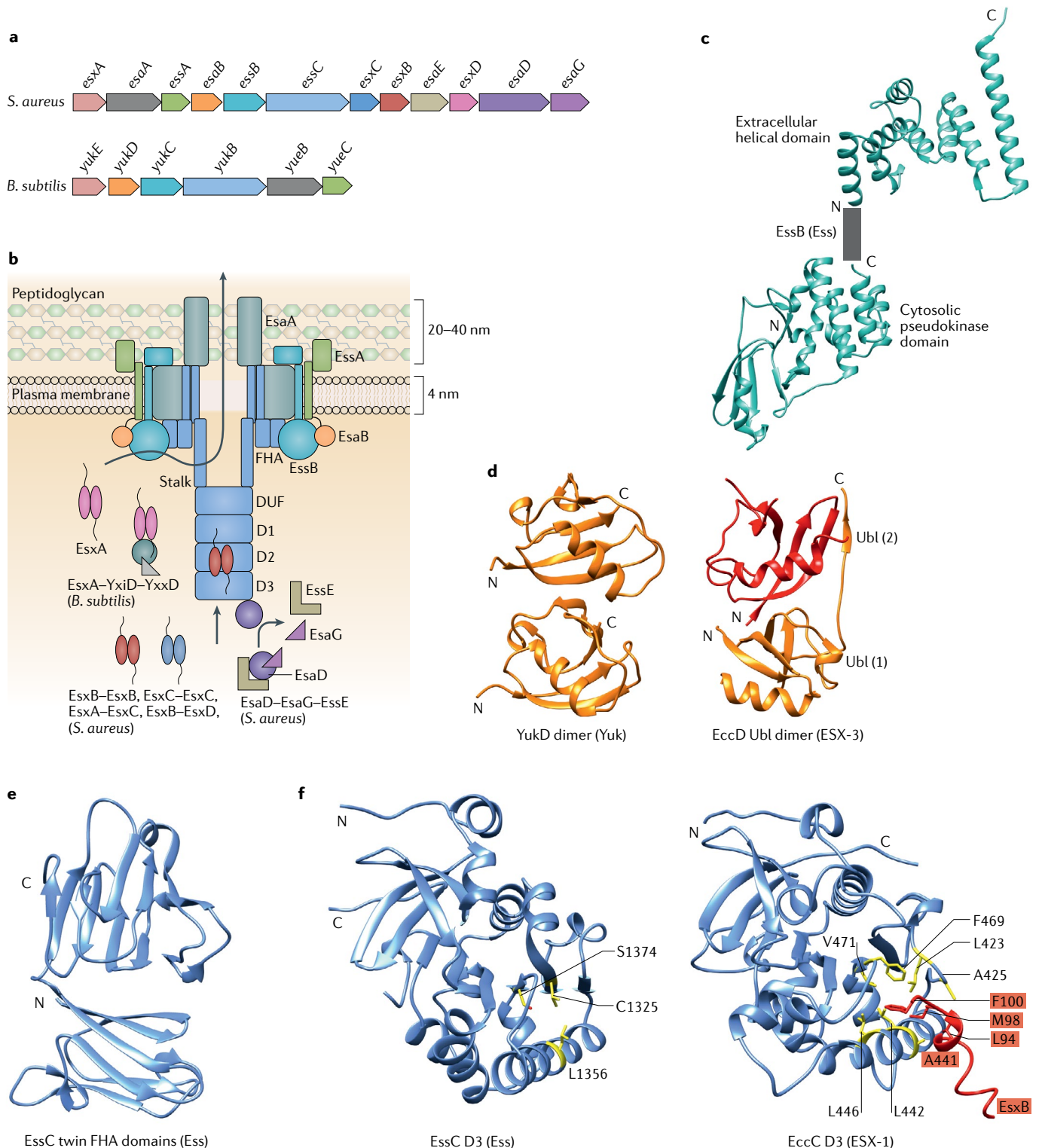
Fig. 3 | Organization of T7SSb and structural comparison with mycobacterial T7SSs. a | Type VII secretion system b (T7SSb) gene clusters of Ess from *Staphylococcus aureus* USA300 and Yuk from *Bacillus subtilis*. b | Functional organization of T7SSb. The membrane proteins EssA, EssB, EssC and EsaA as well as the cytoplasmic protein EsaB assemble the secretion machine in the cell envelope (Ess nomenclature). The EsxA homodimer and the toxin–antitoxin complex YxiD–YxxD are recruited via EssB to the secretion complex, whereas other effector proteins (EsxB, EsxC, EsxD and EsaD) are targeted to EssC. c | Crystal structures of the EssB extracellular domain of Ess from *Geobacillus thermodenitrificans* (Protein Data Bank (PDB) ID 2YNO) and the EssB cytosolic domain of Ess from *S. aureus* (PDB ID 4ANN). EssB is probably involved in substrate targeting and is a unique structural feature of T7SSb. d | The structural comparison between ubiquitin-like domain (Ubl) dimers of YukD from *B. subtilis* (PDB ID 2BPS)¹¹⁰ and EccD of ESX-3/T7SS from *Mycobacterium smegmatis* (PDB ID 6SGX) shows a different monomer–monomer interface. The implications for T7SSb assembly and transport are unclear. e | Crystal structure of the amino-terminal EssC twin FHA domains of Ess from *S. aureus* (PDB ID 1WV3). The twin FHA domains probably couple targeting and transport of a subset of substrates in T7SSb and are a unique structural feature of the T7SSb. f | Structural comparison of the surface-exposed pocket of EssC D3 domain of Ess from *S. aureus* (PDB ID 6TV1) and EccC D3 of ESX-1/T7SS from *Mycobacterium tuberculosis* (PDB ID 6J19). The pocket exhibits hydrophobicity in both systems but little conservation of the amino acid composition. The depicted amino acids (yellow) in the D3 structure of Ess are essential for secretion in *S. aureus*. In D3 of ESX-1 from *M. tuberculosis*, the amino acids participating in the signal peptide–pocket interaction are shown in red and yellow, respectively. C, carboxy terminus; DUF, domain of unknown function; N, amino terminus.

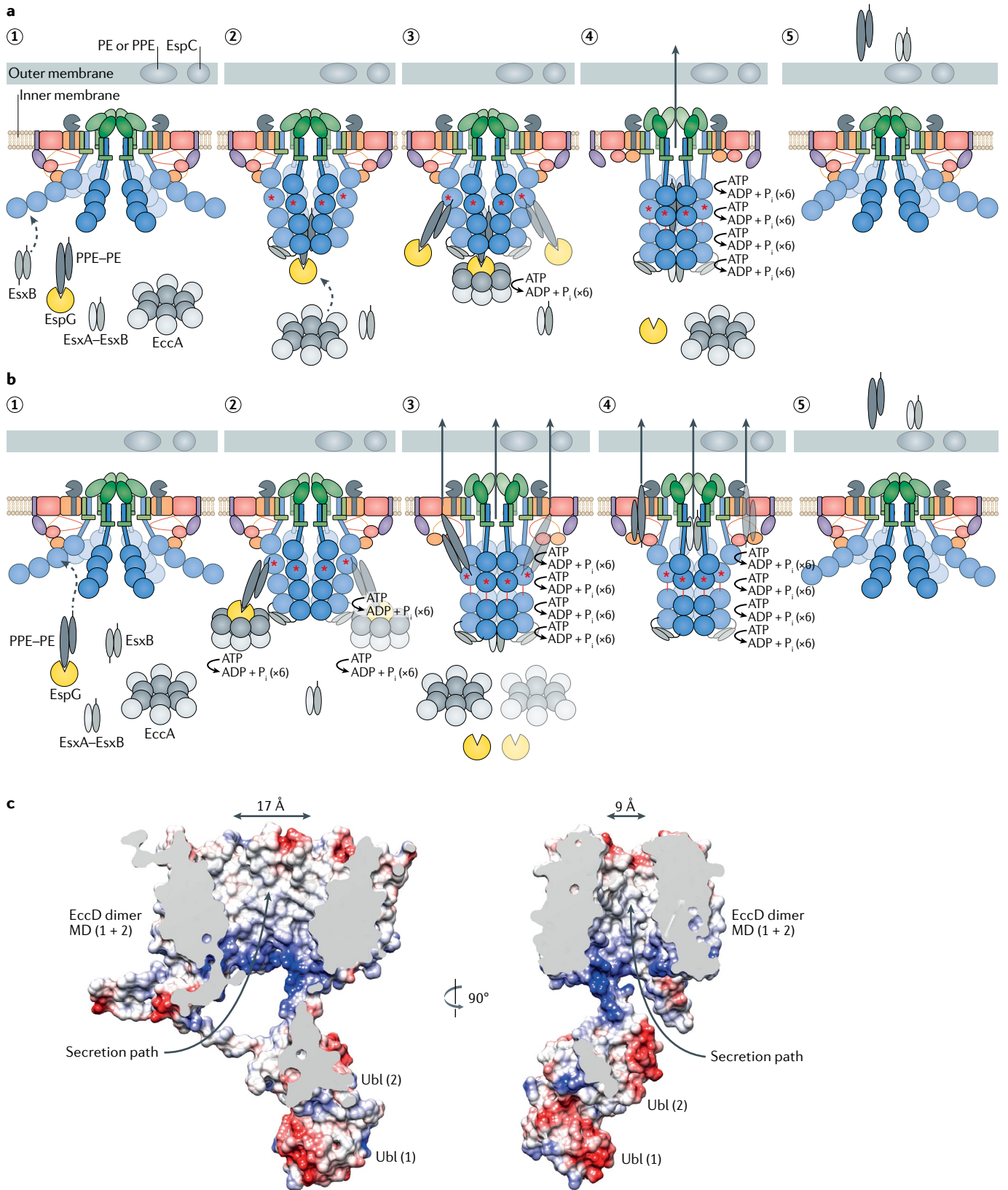
►

Transport models

In the context of the mycobacterial cell wall, substrate proteins must cross the cytoplasmic membrane and an additional mycolate membrane before they are released into the extracellular environment or are inserted into the cell envelope. The secretion mechanism for T7SS substrates is therefore likely to be unique to those members of *Corynebacteriales* that possess an outer membrane, including mycobacteria. Substrates could be first

transported across the cytoplasmic membrane by the T7SS core complex into the periplasmic space and then further secreted into the extracellular environment by a yet unknown T7SS component or independent secretion system. Alternatively, substrates could be secreted in one step from the cytosol directly across both the cytoplasmic membrane and the outer membrane into the extracellular environment. Current structural information shows that the T7SS core complex resides in





the cytoplasmic mycobacterial membrane, thus leaving unresolved how proteins are transported across the periplasmic space and the outer membrane.

Two different transport mechanisms are conceivable for substrate transport across the cytoplasmic membrane

on the basis of the available structural information. In the central pore model, all substrates are transported one after the other in their folded state across a central pore. In the protomer pore model, substrates with the PE-PPE signature are transported across smaller pores within

◀ Fig. 4 | **Transport models of mycobacterial type VII secretion systems.** Two different models for substrate transport across the inner mycobacterial membrane are presented. The common key aspect is the activation of the motor ATPase EccC (blue) by specific substrate interactions inducing oligomerization and abolishing autoinhibition. The cytosolic EccA ATPase is presented as a factor dissociating PE–PPE complexes from their cognate EspG chaperones before transport. In both models, proteins of the PE–PPE family are proposed to form the outer membrane conduit. **a** | In the central pore model, all substrates are targeted to the D3 layer of the motor ATPase and are then secreted through the central ATPase barrel across the membrane pore. Inactive state of the secretion machine (stage 1). Specific substrate interactions activate the motor ATPase (stages 2 and 3). EsxB homodimers trigger oligomerization (stage 2) and binding of PE–PPE substrates to the outside of the ATPase barrel abolishes autoinhibition of D1 (stage 3). The arginine finger crucial for D1 ATPase activity is indicated with a red asterisk. Only when both substrates, EsxB homodimer and PE–PPE, are bound to the ATPase can transport be initiated. Subsequently, substrates of the WXG100 family (for example, the indicated EsxA–EsxB heterodimer) or the PE–PPE family are targeted to the D3 layer. This step is indicated only for PE–PPE substrates in the figure (stage 3). PE–PPE substrates are dissociated from their chaperone EspG (yellow) by the cytosolic EccA ATPase (grey). Formation of the ATPase barrel and ATP hydrolysis opens the membrane and exit pore, enabling transport across the inner membrane (stage 4). When substrate levels in the cytoplasm are decreasing, substrates dissociate from the barrel and the motor ATPase returns to its inactive tentacle-like state (stage 5). **b** | In the protomer pore model, PE–PPE substrates are translocated through hydrophobic pores in the protomers, while WXG100 substrates are transported across the central pore. Inactive state of the secretion machine (stage 1). Loading of the EsxB homodimer to D3 triggers oligomerization of the motor ATPase (stage 2). PE–PPE–EspG complexes are loaded to linker 2. EccA dissociates PE–PPE complexes from the chaperone EspG during loading. PE–PPE substrates are inserted with their hydrophobic tip into the EccD pore, while WXG100 substrates (for example, EsxA–EsxB as indicated in the figure) enter the ATPase barrel (stage 3). The movement of DUF (domain of unknown function) or D1 could push PE–PPE substrates through the EccD pore (stages 4 and 5). **c** | The cross section and coulombic surface colouring of the EccD dimer shown in isolation illuminates the hydrophobic interior of the EccD pore. Grey indicates near neutral or hydrophobic potential¹⁴, blue indicates electropositive potential and red indicates electronegative potential. Arrows indicate possible routes for entering the EccD pore. MD, membrane domain; Ubl, ubiquitin-like domain.

each protomer, whereas substrates of the WXG100 family are transported through the central pore. Transport through the protomer pore requires the dissociation of substrate dimers or even their partial unfolding and allows the simultaneous transport of substrates by different protomers in the hexameric assembly. These models are currently hypothetical, and further work will be needed to improve our understanding of T7SS transport.

Central pore model. The activation of the coupling protein likely requires the loading of two disparate substrate-binding sites to abolish autoinhibition and promote oligomerization^{90,117}. This requirement could explain the phenomenon of codependent secretion of effector protein complexes, in which the absence of one substrate pair abolishes secretion of another substrate pair (FIG. 4a).

The first binding site is a hydrophobic pocket on D3 that interacts with hydrophobic residues on the C-terminal signal peptide of EsxB, but not with the YXXXD/E motif^{90,93} (FIG. 2e). In vitro experiments on EccC from *T. curvata* have shown that an EsxB homodimer is able to promote EccC oligomerization but is not sufficient to trigger its ATPase activity, and that ATPase activity requires an additional allosteric activation event⁹⁰. The requirement for oligomerization can be explained by the presence of an arginine finger on neighbouring D1 protomers that is thought to complete the nucleotide-binding pockets of the ATPase domain in the oligomeric state. By contrast, EsxA homodimers

antagonize EccC oligomerization⁹⁰. These findings suggest that substrate-controlled oligomerization could regulate EccC activity. In *M. tuberculosis*, EsxA and EsxB homodimers have not been described but it is known that low pH and post-transcriptional acetylation of EsxA can disrupt the EsxA–EsxB heterodimer and perhaps initiate homodimerization^{118,119}.

A second putative binding site was recently discovered on linker 2 of EccC (FIG. 2c,d). A small stretch on linker 2 is required for species-specific secretion of PE–PPE substrates, indicating interaction with these substrates or with the chaperone EspG, which targets PE–PPE to the secretion machine¹¹⁷. Substrate or chaperone binding could lead to the displacement of linker 2 from the D1 pocket and thus allosterically activate D1.

Linker 2 localizes outside the vestibule structure. It is conceivable that a portion of the cytosolic PE–PPE–EspG population must interact with linker 2 outside the vestibule to activate the secretion machine before substrate transport across the central pore can occur. There is also a possibility that substrate binding to linker 2 precludes PE–PPE transport across the central pore and requires an alternative transport model (see the section entitled ‘Protomer pore model’). During activation, the motor ATPase probably undergoes a transformation from the extended configuration via a vestibule-like intermediate structure into the active ATPase barrel, which requires large structural rearrangements of D1 and DUF. The displacement of DUF from its positions next to the Ubl anchoring platform in combination with its ATPase activity could trigger the opening of the membrane pore as DUF and the EccC TMH are connected through a stalk domain and permit substrate transport across the inner membrane. Transport would be terminated when decreasing substrate concentrations cause the dissociation of substrates from their binding sites on linker 2 or D3 in the cytoplasm, resetting the motor ATPase to its tentacle-like configuration.

The cryo-EM structure of ESX-5 from *M. tuberculosis* shows that substrates that are translocated through the central membrane pore must also pass through the EccB–MycP dome⁴³. The subtilisin-like serine protease MycP active sites face the inside of the dome-like structure, suggesting that MycP selectively processes substrates that contain a MycP cleavage site^{43,87,120,121}. However, the proteolytic activity of MycP is not essential for secretion, and only a single processed ESX-1 secreted protein, EspB, has been identified so far as a substrate^{122,123}. Thus, the primary role of MycP is to act as an allosteric driver for EccB hexamerization, as evidenced in the recent cryo-EM structure of ESX-5 from *M. tuberculosis*, thus further stabilizing the hexameric state of the ESX membrane complex^{43,124}.

The interaction of the accessory components EspG and EccA with the membrane-embedded secretion machine is not understood. The cytosolic chaperone EspG shows a mixed α – β -fold and binds the hydrophobic tip of the PPE protein, preventing aggregation of the PE–PPE pair^{125,126}. Therefore EspG chaperones have a crucial role in targeting substrate dimers with a PE–PPE signature to their cognate secretion machine^{125,127}. Although EspG does not interact with Esx substrates,

a recent *in vivo* study showed that EspG also determines the system specificity of the Esx substrate family in a manner that is not yet understood¹²⁸. Comparison of PE–PPE–EspG structures indicates that shape complementarity between EspG and PPE enables EspG to discriminate between cognate and non-cognate substrates¹²⁹. Unloading of PE–PPE to the targeting site could be facilitated by transitioning between two known EspG conformations and aided by the cytosolic ATPase EccA¹²⁹, which is required for secretion of a specific subset of substrates and may be recruited to the ESX secretion machine upon substrate binding³⁸. Six EccA tandem tetratricopeptide repeat domains could mediate the known interactions with EspG and PPE, while the C-terminal AAA+ ATPase domain could provide the energy for dissociating PE–PPE from EspG^{39,125,130}.

Instigator model. The instigator transport model is a variant of the central pore model, in which EccA acts as an instigator of secretion⁴¹. As ATP hydrolysis of D2 and D3 in EccA has probably a minor contribution to the overall secretion activity, it raises the question of how substrates pass to the more active D1 ATPase ring layer. It has been speculated that the EccA tetratricopeptide repeat domain is loaded with Esx substrates and the ATPase activity of EccA provides the energy for ‘pushing’ the loaded Esx substrates into the ATPase barrel. Finally, EccA hexamers and the D3 hexameric model are predicted to have compatible dimensions. Binding of EccA could stabilize the active hexameric conformation of D3 and thereby increase secretion activity. However, it is important to note that not all secreted substrates require EccA for transport and that the impact of EccA on transport appears to be regulated by specific environmental conditions^{38,40}.

Protomer pore model. In an alternative secretion model, the EccD dimers are proposed to serve as secretion pores in all six protomers⁴⁴ (FIG. 4b). The elliptical shape of the EccD pore would require dissociation of substrate dimers along with partial unfolding or a major conformational change of the EccD pore. The interior of the EccD pore is almost entirely hydrophobic and plugged with lipids, visible as disordered density inside the pore of the cryo-EM maps, which makes it unlikely that substrates with a hydrophilic surface could pass through (FIG. 4c). PPE substrates could be inserted with their hydrophobic tip into the EccD cavity but would need to expel the lipids inside the pore. The insertion of substrates could prime the EccD pore for transport by inducing conformational changes. The putative binding site for PE–PPE complexes on linker 2 localizes near the cytosolic entry site of the EccD pore (FIGS 2c,d,4c), and the EccC DUF domain or D1 domain could create a motion in the direction of the EccD pore (FIG. 4b). In this model, the transport of six PE–PPE complexes occurs simultaneously with one Esx substrate pair transported across the central pore.

Transport across the outer membrane. Current structural knowledge indicates that ESX membrane core complexes do not reach the mycomembrane. Thus, this could imply a two-step transport mechanism, first transport into the periplasm and then secretion into the extracellular

environment by a hitherto unidentified outer membrane pore. Alternatively, additional periplasmic components could span the periplasm, allowing substrate secretion from the cytosol in one step into the extracellular environment.

Although the outer membrane pore for T7SS protein export is unknown, a recent study showed that a subset of PE–PPE proteins form porins in the outer membrane and enable the selective uptake of small molecules such as cations (magnesium; PE20–PPE31), anions (phosphate; PE32–PPE65) or carbon sources (that is, glucose; PE19–PPE51)¹³¹. Given the large number of PE and PPE proteins (169 orthologues) and their frequent association with the mycomembrane, these proteins are candidates for assembling substrate pores in the mycomembrane.

The protein EspC, although not initially identified as a PE protein, was later shown to contain a PE motif and was proposed to act as an outer membrane conduit because it polymerizes into a needle-like structure¹³². A needle could transport substrates through a lumen. Further research is needed to show whether EspC spans the mycomembrane and whether the needle contains a lumen for transport. EspB has been discussed as an outer membrane pore on the basis of a low-resolution structure of the EspB heptamer¹³³. However, recent high-resolution cryo-EM structures revealed a large (45 Å), unplugged pore with an electronegative exterior, precluding insertion into the hydrophobic outer membrane^{134,135}. Instead, the EspB heptamer could be connected to the periplasmic exit site of the core complex to enable directed transport across the periplasm, or it could be docked to an unknown outer membrane pore to mediate transition through the capsule^{134,135}. An electropositive patch in the barrel lumen of the heptameric EspB is consistent with the reported binding of phospholipids and with its essential function in DNA uptake by the recipient strain (in *M. smegmatis*), and supports suggested roles of EspB in scavenging important signalling lipids or in DNA transport across the capsule^{134–136}. EspC and EspB are specific substrates of ESX-1. Homologues with analogous properties have not been identified yet in other ESX systems.

Flexibility. The available structures of T7SSs reveal that flexibility is an inherent property of this secretion system. EccC is inherently flexible, as first revealed in the negative-stain electron microscopy structure of ESX-5 from *M. xenopi* and by small-angle X-ray scattering analysis of monomeric EccC⁸⁷. The recent cryo-EM structures of ESX-3 from *M. smegmatis* provided further evidence of intrinsic flexibility at two key regions of the T7SS core complex: the distal region in EccC involved in substrate recognition and EccB. Recent cryo-EM structures of ESX-5 from *M. tuberculosis* and *M. xenopi* further confirm this flexibility^{42,43}. Both EccB and EccC have key roles in the central pore model of secretion, in which conformational changes in EccC upon substrate binding are propagated along EccC, including the stalk domain, which contacts the cytoplasmic tail of EccB, allowing the rearrangement of the EccC TMH bundle and opening of the membrane pore. The fork-like structure formed by the EccB dimer is symmetrical and rigid, and holds two protomers together, but its attachment

3D variability analysis

A tool to analyse the heterogeneity in single-particle cryogenic electron microscopy data sets revealing the different 3D conformations that appear in the sample. It can be used to characterize the conformational space and the amount of flexibility present in a molecule.

Pyroptosis

Type of programmed cell death different from apoptosis and necroptosis that promotes lytic cell death, causing the release of the cellular content and inducing inflammatory responses in the organism.

to the cytoplasmic membrane exhibits a high degree of flexibility, allowing EccB dimers to adopt different configurations in the hexameric assembly, as revealed by the recent cryo-EM structures of ESX-5 (REFS^{42,43}).

To characterize in greater detail the flexibility of ESX-3, we performed a 3D variability analysis (3DVA)^{137,138} of ESX-3 cryo-EM images³⁷. This analysis resolved a number of discrete subsets of cryo-EM images corresponding to molecules with different conformations coexisting in samples. The results reveal the extraordinary flexibility in the distal regions of EccC and suggest that periplasmic flexibility of the EccB dimer exerts major forces on the inner membrane complex, triggering a tweezer-like motion of the two ESX protomers (Supplementary Video 1). This intradimeric angular variation observed among the ESX-3 resolved states now extends to the cryo-EM structure of hexameric ESX-5, where increased intradimeric and interdimeric angle heterogeneity for particles that lack a MycP-stabilizing effect was noted^{42,43}. Furthermore, variability analysis performed on the cryo-EM images of ESX-3 also suggested a certain degree of correlation between the conformations of EccB and EccC (Supplementary Videos 1,2). This agrees with the central pore model of secretion, which relies on the direct communication between EccB and EccC.

In summary, two main transport mechanisms are discussed for the transport of substrates across the cytoplasmic membrane; however, substrate export across the outer membrane is not understood. It has become clear that some secreted proteins of the PE–PPE class can form porins in the outer membrane for nutrient uptake. We speculate that the same protein class could form a secretion pore for substrate proteins in the outer membrane. The protomer pore model proposes the simultaneous transport of the PE–PPE substrate class across the six protomers and of WXG100 substrates across the central pore.

Functions of effector proteins

T7SSs are conserved across diverse phyla, which underlines their role in bacterial fitness and survival, and are involved in diverse biological processes, among which pathogenicity stands out. Indeed, the contribution of ESX systems to key aspects of *M. tuberculosis* pathogenicity (for example, host cell modulation and phagosome rupture) is well established¹³⁹.

Defining the specific contribution of the different effectors to biological functions is hampered owing to the codependent nature of T7SS substrate secretion. The phenomenon of codependency is evident in pairs of substrates that are secreted as heterodimers (BOX 1), but it also extends to pairs of substrates that require different pair of substrates for their secretion.

Pathogenesis, evasion of immunity, nutrient uptake and host interactions. Progression of mycobacterial infection leading to tuberculosis is enabled by virulence factors secreted by the T7SS machineries, which are involved at all stages of infection, from host colonization to persistence (FIG. 5). *M. tuberculosis* is commonly spread through respiratory aerosols. The inhaled bacilli are engulfed by macrophages in the alveoli or invade the airway mucosa aided by ESX-1 (REF.¹⁴⁰). Inside the macrophage, ESX-1 has

a crucial role in the survival of *M. tuberculosis* by enabling the escape from the phagosome^{141,142}. ESX-1 causes damage to the phagosomal membrane, which increases as infection progresses, allowing delivery of effectors to the cytosol, access to cytosolic nutrients and eventually translocation to the cytosol, favouring bacterial replication¹⁴³. An initially suggested membrane-disruption role of the secreted ESX-1 substrate EsxA has been questioned^{118,144,145}. Instead, contact-dependent cell lysis has been reported¹⁴⁴, and the cell surface-associated lipid phthiocerol was found to act in concert with ESX-1 to induce phagosomal rupture^{60,146}. The ESX-1 membrane-damaging activity is not restricted to the phagosome, and damage to the host cytoplasmic membrane during *M. tuberculosis* infection can trigger pyroptosis and facilitate the dissemination of bacteria into the environment⁶².

The membranolytic activity of ESX-1 leads to the recruitment of the endosomal sorting complex required for transport (ESCRT) machinery to phagosomes containing *M. tuberculosis*⁵⁸. The ESCRT machinery is involved in membrane remodelling functions such as the repair of damaged endolysosomes¹⁴⁷. The ESX-3 substrate EsxH antagonizes membrane repair through binding to the HGS (also known as HRS) component of the ESCRT machinery⁵⁶. Further consequences of ESCRT targeting by EsxH include impairment of phagosome maturation and fusion with the lysosomes and suboptimal antigen processing, which compromises MHC class II antigen presentation by macrophages and dendritic cells and consequently interferes with the activation of CD4⁺ T helper cells⁵⁷.

It has been proposed that ESX-1-mediated phagosomal escape into the cytosol causes leakage of bacterial DNA into the host cell cytosol¹⁴⁸. The exogenous DNA is sensed by cyclic GMP–AMP (cGAMP) synthase (cGAS)^{145,149–151}. Second-messenger cGAMP signalling activates the stimulator of interferon genes (STING) pathway in the host cell as well as in neighbouring cells, leading to production of type I interferons, which is accompanied by increased host cell necrosis and tissue damage promoting dissemination of mycobacteria into the host environment. This working model has recently been challenged, and it has been proposed that DNA (both nuclear and mitochondrial) in the host cell activates the cGAS–STING pathway instead of the mycobacterial DNA, while a separate ESX-1 function is responsible for releasing host DNA¹⁴⁵.

ESX-1 also has an important role in triggering a multi-cellular immune response resulting in the formation of granulomas, clusters of immune cells that surround infected cells. Granulomas can be exploited by *M. tuberculosis* as replication niches or for long-term persistence until reactivation causes outbreak and dissemination to other organs^{152–156}.

Throughout the infection, T7SS proteins are involved in nutrient uptake. A subset of PE–PPE proteins form porins in the mycomembrane for the selective uptake of small molecules^{50,131}. Indeed ESX-3-mediated and ESX-5-mediated nutrient uptake is essential for mycobacterial viability^{50,54,55}, and ESX-3 is specifically involved in the acquisition of Fe²⁺ and haem^{54,55,157}. Although macrophages are rich iron sources due to their function in

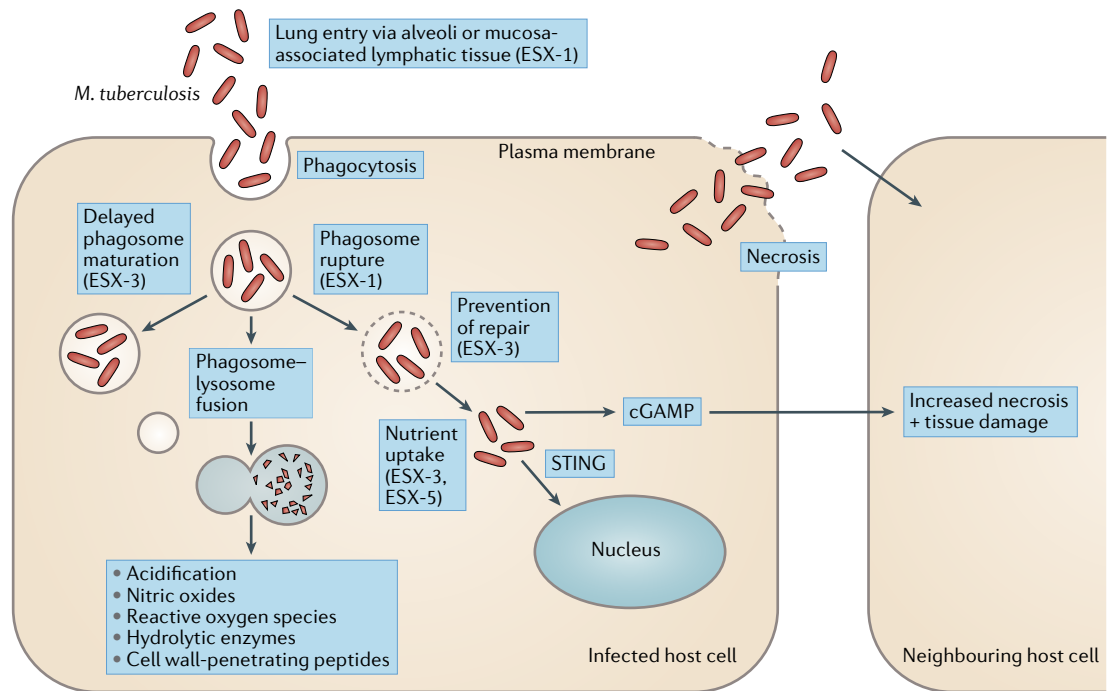


Fig. 5 | Roles of mycobacterial type VII secretion systems in the pathogenesis of tuberculosis. The infection route for the most prevalent pulmonary form of tuberculosis is depicted and the roles of type VII secretion systems are indicated. Upon entry into the lung, *Mycobacterium tuberculosis* is engulfed by macrophages in the alveoli (ESX-1), and its survival depends on the successful interference with phagocytosis. *M. tuberculosis* delays the fusion of the phagosome to the lysosome (ESX-3), preventing the formation of phagolysosomes, which would degrade *M. tuberculosis*. The various processes that contribute to the harsh environment found in the phagolysosomes are indicated. Type VII secretion systems are key in promoting phagosome rupture (ESX-1) but also in preventing phagosome membrane damage repair (ESX-3). Phagosome lysis enables escape into the cytoplasm, resulting in the gaining of access to a nutrient-rich growth environment and favouring bacterial replication. Nutrient uptake is mediated by ESX-3 and ESX-5. *M. tuberculosis* infection activates the cyclic GMP–AMP (cGAMP) synthase (cGAS)–stimulator of interferon genes (STING) pathway, which promotes host cell necrosis and tissue damage and favours the spread of the pathogen in the host.

recycling iron from proteins and haem, the availability of free iron in the cytosol is restricted by ferritin iron storage cages¹⁵⁸. Outside the macrophage, iron or haem iron is primarily bound by iron-binding or haem-binding proteins (for example, lactoferrin, transferrin, haptoglobin, haemopexin and albumin)¹⁵⁸. To counter iron restriction, *M. tuberculosis* uses two iron-scavenging siderophores, mycomembrane-associated mycobactin and soluble carboxymycobactin¹⁵⁸. The ESX-3 protein PPE4 translocates to the mycomembrane, where it mediates uptake of ferric carboxymycobactin in an unknown manner⁵³.

ESX-5 mediates the uptake of fatty acids and other nutrients⁵⁰. The PE substrate LipY is a triacylglycerol lipase with a central role in triacylglycerol metabolism involved in the degradation of extracellular and intracellular lipids upon carbon deprivation¹⁵⁹. LipY plays an important role in exiting the dormancy stage in the granuloma environment, in which *M. tuberculosis* relies on free fatty acids as a carbon source¹⁵⁴.

DNA transfer. DNA exchange is a major driving force for evolution and diversification in bacteria. Chromosomal DNA transfer among strains of *Mycobacterium canettii*, a tuberculosis-causing mycobacterium closely related to *M. tuberculosis*, has been described¹⁶⁰. The mechanism underlying the genomic exchange is currently unknown, but it is responsible for the mosaic arrangement

in *M. canettii* genomes, a feature also observed in *M. smegmatis* genomes¹⁶⁰. Indeed, *M. smegmatis* is able to perform genomic exchange between different strains in an ESX-1-dependent and ESX-4-dependent manner in a process called ‘distributive conjugal transfer’ (DCT)^{65,161–163}. Both systems are required for DCT in the recipient cell, whereas in the donor strain, *esx-1* mutants exhibit a hyperconjugative phenotype and *esx-4* mutants perform DCT normally^{65,164}. During DCT, a donor strain is detected by the recipient cell, which induces *esx-4* expression in an ESX-1-dependent manner in the recipient strain, enabling the acquisition of donor DNA. ESX-1 is proposed to mediate the secretion of mating identity (*mid*) proteins that determine mating identity, which is consistent with the presence of the *mid* locus in *esx-1* (REF.¹⁶²). The role of ESX-4 in DCT is less well defined, and it was suggested to mediate cell wall remodelling to favour DNA transfer, or even secrete structural components that could assemble the channel through which DNA is internalized. DCT, therefore, relies on the unexpected cooperativity of two different ESX systems¹⁶⁵.

DNA transfer is not mediated exclusively by ESX-1 and ESX-4 in *M. smegmatis*. ESX-P1 is a newly identified T7SS present in the conjugative plasmid pRAW from *M. marinum* and is essential for the conjugal transfer of this plasmid²⁸. ESX-P1 exhibits closest homology with the ESX-5 system¹⁶⁶, and the ESX-P1 locus includes two

distinctive genes encoding peptidoglycan-associated glycoside hydrolases²⁸. Interestingly, the pRAW plasmid also contains genes homologous to components of the type IV secretion system (T4SS), including the ATPase VirB4 and relaxase. Indeed, the conjugal transfer of pRAW depends on components from both types of secretion system, the ESX-P1 system and the T4SS-like system²⁸.

Cell envelope. ESX substrates have been found to be localized to the mycobacterial cell surface and associated with the capsule¹⁶⁷. ESX-1 and ESX-5 effectors have profound effects on cell wall properties. ESX-1 activity affects mycobacterial colony morphology²² and cell wall stability in a way that is yet to be understood¹⁶⁸, and ESX-5 activity affects the permeability of the cell envelope, in line with the described porin function of some of its PE–PPE substrates^{50,131}. The ESX-5 substrate PPE10 is required for capsule integrity and virulence¹⁶⁹, and many PE–PPE proteins transported by ESX-5 remain in the cell envelope, where they are perfectly placed to mediate host–pathogen interactions or to perform immunomodulatory functions⁵⁰.

Bacterial competition, spore formation and development and phage infection (T7SSb). T7SS effectors do not only target eukaryotic hosts. Recent research shows that the Firmicutes members *S. aureus*, *B. subtilis* and *Streptococcus intermedius* have the ability to kill bacterial competitors in a T7SSb-dependent manner. Several secreted proteins were identified that belong to the polymorphic (F/L)XG toxin family^{97–100}. For example, EsaD is a nuclease toxin secreted by the staphylococcal T7SSb into the extracellular environment¹⁰⁰. The toxin TspA is widespread across *S. aureus* strains and *Listeria* and *Enterococcus* species. TspA associates with the cell envelope of *S. aureus* and exhibits a membrane-depolarizing activity that it exerts on prey bacteria⁹⁷. A recent preliminary study indicates that the cell envelope-spanning T7SSb secretion apparatus itself has bactericidal activity and exhibits membranolytic activity¹¹⁶.

T7SSb effectors have also been implicated in spore formation and development in *Streptomyces coelicolor*¹⁷⁰. Interestingly, these effectors act intracellularly, probably affecting developmental programmes, although the detailed mode of action is currently unknown.

A recent study found that T7SSb genes are activated in response to phage infection in *Enterococcus faecalis*^{171,172}. This activation could be part of the stress response as a result of the cell membrane damage induced by the phage infection similar to the role of T7SSb in *S. aureus* membrane homeostasis¹⁷³.

Conclusions and perspectives

The rise in multidrug-resistant tuberculosis cases necessitates the development of novel antibacterial strategies. Bacterial virulence factors such as protein secretion systems have only recently been explored as potential antibacterial drug targets^{174–176}.

Two chemical classes, benzothiofenenes and benzyloxy benzylidene hydrazines, were found to inhibit ESX-1 secretion and significantly increase survival of lung fibroblast in vitro¹⁷⁷. ESX-1 is primarily responsible

for the attenuation of the vaccine strain *M. bovis* BCG and has key functions in phagolysosomal escape and in host cell lysis, promoting pathogen spreading inside the host. Compromising ESX-1 function could therefore control infection or create a window of opportunity for the immune system to clear the pathogen. ESX-3 and ESX-5 may also become important drug targets as both systems have functions in nutrient uptake that are crucial for mycobacterial growth. Therefore, inhibiting ESX-3 and ESX-5 might have a bacteriostatic effect, preventing the spread of infection. Such tailored treatment is likely to cause less collateral damage to the human microbiota than conventional antibiotics that non-specifically inhibit essential biological functions (protein translation, transcription or cell wall biogenesis).

In recent years, important progress has been made towards a mechanistic understanding of T7SSs. Investigations into the interplay of substrates with the T7SS secretion machine have provided the first insights into the substrate specificity of T7SSs and revealed essential requirements for transport. The elucidation of the negative-stain electron microscopy structure of the ESX-5 core complex hexamer and the cryo-EM structure of the ESX-3 core complex in the dimeric state enabled the generation of the first structural model of the T7SS. This structural model has been confirmed by recent cryo-EM structures of ESX-5 from *M. tuberculosis* and *M. xenopi*, revealing the versatility of the periplasmic region and the detailed configuration of the central pore. It has become apparent that the inherent flexibility of these machines is functionally relevant to the substrate transport mechanism and poses a great challenge for future structural studies that aim to provide a deeper mechanistic understanding of T7SSs, at best in different transport states (inactive, closed and active, open).

Recent structural data have revealed two possible transport mechanisms across the cytoplasmic membrane that need to be tested and validated. An unresolved question is how accessory components and substrates are involved in the secretion process: how do they activate the secretion machine? Is the cytosolic ATPase EccA an instigator of secretion or a factor in dissociating chaperones from substrates before transport? How do chaperone–substrate complexes recognize their cognate secretion machine? How is the proteolytic activity of MycP synchronized with substrate transport?

The localization of the core complex in the mycobacterial inner membrane raises the question of how effector proteins are exported through the periplasm and the outer mycobacterial membrane. The answer to this question has implications for the transport mechanism: a cell envelope-spanning structure would enable substrate transport into the extracellular environment in one step, which could be fuelled by ATP in the cytoplasm. A distinct organization of the T7SS in an inner membrane and an outer membrane complex would result in a two-step mechanism with substrate release into the periplasm, requiring a different energy source for transport across the outer membrane because ATP is not available in the periplasm.

Published online 26 May 2021

1. Green, E. R. & Meccas, J. Bacterial secretion systems: an overview. *Microbiol. Spectr.* **4**, VMBF-0012–VMBF-2015 (2016).
2. Andersen, P., Andersen, A. B., Sorensen, A. L. & Nagai, S. Recall of long-lived immunity to *Mycobacterium tuberculosis* infection in mice. *J. Immunol.* **154**, 3359–3372 (1995).
3. Gerlach, R. G. & Hensel, M. Protein secretion systems and adhesins: the molecular armory of Gram-negative pathogens. *Int. J. Med. Microbiol.* **297**, 401–415 (2007).
4. Winstanley, C. & Hart, C. A. Type III secretion systems and pathogenicity islands. *J. Med. Microbiol.* **50**, 116–126 (2001).
5. Costa, T. R. et al. Secretion systems in Gram-negative bacteria: structural and mechanistic insights. *Nat. Rev. Microbiol.* **13**, 343–359 (2015).
6. Rapisarda, C., Tassinari, M., Gubellini, F. & Fronzes, R. Using cryo-EM to investigate bacterial secretion systems. *Annu. Rev. Microbiol.* **72**, 231–254 (2018).
7. Palmer, T., Finney, A. J., Saha, C. K., Atkinson, G. C. & Sargent, F. A holin/peptidoglycan hydrolase-dependent protein secretion system. *Mol. Microbiol.* **115**, 345–355 (2021).
8. Abby, S. S. et al. Identification of protein secretion systems in bacterial genomes. *Sci. Rep.* **6**, 23080 (2016).
9. Erhardt, M., Namba, K. & Hughes, K. T. Bacterial nanomachines: the flagellum and type III injectisome. *Cold Spring Harb. Perspect. Biol.* **2**, a000299 (2010).
10. Ho, B. T., Dong, T. G. & Mekalanos, J. J. A view to a kill: the bacterial type VI secretion system. *Cell Host Microbe* **15**, 9–21 (2014).
11. Kühlbrandt, W. The resolution revolution. *Science* **343**, 1443–1444 (2014).
12. Paulson, T. Epidemiology: a mortal foe. *Nature* **502**, S2–S3 (2013).
13. Berthet, F. X., Rasmussen, P. B., Rosenkrands, I., Andersen, P. & Gicquel, B. A *Mycobacterium tuberculosis* operon encoding ESAT-6 and a novel low-molecular-mass culture filtrate protein (CFP-10). *Microbiology* **144**, 3195–3203 (1998).
14. Cole, S. T. et al. Deciphering the biology of *Mycobacterium tuberculosis* from the complete genome sequence. *Nature* **393**, 537–544 (1998).
15. Gey Van Pittius, N. C. et al. The ESAT-6 gene cluster of *Mycobacterium tuberculosis* and other high G+C Gram-positive bacteria. *Genome Biol.* **2**, RESEARCH0044 (2001).
16. Teakaia, F. et al. Analysis of the proteome of *Mycobacterium tuberculosis* in silico. *Tuber. Lung Dis.* **79**, 329–342 (1999).
17. Bitter, W. et al. Systematic genetic nomenclature for type VII secretion systems. *PLoS Pathog.* **5**, e1000507 (2009).
18. Harboe, M., Oettinger, T., Wiker, H. G., Rosenkrands, I. & Andersen, P. Evidence for occurrence of the ESAT-6 protein in *Mycobacterium tuberculosis* and virulent *Mycobacterium bovis* and for its absence in *Mycobacterium bovis* BCG. *Infect. Immun.* **64**, 16–22 (1996).
19. Mahairas, G. G., Sabo, P. J., Hickey, M. J., Singh, D. C. & Stover, C. K. Molecular analysis of genetic differences between *Mycobacterium bovis* BCG and virulent. *M. bovis*. *J. Bacteriol.* **178**, 1274–1282 (1996).
20. Lewis, K. N. et al. Deletion of RD1 from *Mycobacterium tuberculosis* mimics bacille Calmette–Guerin attenuation. *J. Infect. Dis.* **187**, 117–123 (2003).
21. Hsu, T. et al. The primary mechanism of attenuation of bacillus Calmette–Guerin is a loss of secreted lytic function required for invasion of lung interstitial tissue. *Proc. Natl Acad. Sci. USA* **100**, 12420–12425 (2003).
22. Pym, A. S., Brodin, P., Brosch, R., Huerre, M. & Cole, S. T. Loss of RD1 contributed to the attenuation of the live tuberculosis vaccines *Mycobacterium bovis* BCG and *Mycobacterium microti*. *Mol. Microbiol.* **46**, 709–717 (2002).
23. Brodin, P., Rosenkrands, I., Andersen, P., Cole, S. T. & Brosch, R. ESAT-6 proteins: protective antigens and virulence factors? *Trends Microbiol.* **12**, 500–508 (2004).
24. Stanley, S. A., Raghavan, S., Hwang, W. W. & Cox, J. S. Acute infection and macrophage subversion by *Mycobacterium tuberculosis* require a specialized secretion system. *Proc. Natl Acad. Sci. USA* **100**, 13001–13006 (2003).
25. Desvaux, M., Hebraud, M., Talon, R. & Henderson, I. R. Secretion and subcellular localizations of bacterial proteins: a semantic awareness issue. *Trends Microbiol.* **17**, 139–145 (2009).
26. Abdallah, A. M. et al. Type VII secretion—mycobacteria show the way. *Nat. Rev. Microbiol.* **5**, 883–891 (2007).
27. Newton-Foot, M., Warren, R. M., Sampson, S. L., van Helden, P. D. & Gey van Pittius, N. C. The plasmid-mediated evolution of the mycobacterial ESX (Type VII) secretion systems. *BMC Evol. Biol.* **16**, 62 (2016).
28. Ummels, R. et al. Identification of a novel conjugative plasmid in mycobacteria that requires both type IV and type VII secretion. *mBio* **5**, e01744–14 (2014).
29. Dumas, E. et al. Mycobacterial pan-genome analysis suggests important role of plasmids in the radiation of type VII secretion systems. *Genome Biol. Evol.* **8**, 387–402 (2016).
30. Sutcliffe, I. C. New insights into the distribution of WXG100 protein secretion systems. *Antonie van Leeuwenhoek* **99**, 127–131 (2011).
31. Unnikrishnan, M., Constantinidou, C., Palmer, T. & Pallen, M. J. The enigmatic Esx proteins: looking beyond mycobacteria. *Trends Microbiol.* **25**, 192–204 (2017).
32. Abdallah, A. M. et al. A specific secretion system mediates PPE41 transport in pathogenic mycobacteria. *Mol. Microbiol.* **62**, 667–679 (2006).
33. Brodin, P. et al. Dissection of ESAT-6 system 1 of *Mycobacterium tuberculosis* and impact on immunogenicity and virulence. *Infect. Immun.* **74**, 88–98 (2006).
34. Houben, E. N. et al. Composition of the type VII secretion system membrane complex. *Mol. Microbiol.* **86**, 472–484 (2012).
This study provides the first biochemical evidence that EccB–EccF form a secretion complex in the mycobacterial cell wall.
35. Ohl, Y. M. et al. *Mycobacterium tuberculosis* MypP1 protease plays a dual role in regulation of ESX-1 secretion and virulence. *Cell Host Microbe* **7**, 210–220 (2010).
36. Siegrist, M. S. et al. Mycobacterial Esx-3 requires multiple components for iron acquisition. *mBio* **5**, e01073–01014 (2014).
37. Famelis, N. et al. Architecture of the mycobacterial type VII secretion system. *Nature* **576**, 321–325 (2019).
This study shows the first high-resolution structure of the ESX-3 core complex in the dimeric state, revealing the protomer architecture, and enabled the generation of the first structural model for T7SS secretion complexes in the inner membrane.
38. Champion, P. A., Champion, M. M., Manzanillo, P. & Cox, J. S. ESX-1 secreted virulence factors are recognized by multiple cytosolic AAA ATPases in pathogenic mycobacteria. *Mol. Microbiol.* **73**, 950–962 (2009).
39. Teutschbein, J. et al. A protein linkage map of the ESAT-6 secretion system 1 (ESX-1) of *Mycobacterium tuberculosis*. *Microbiol. Res.* **164**, 253–259 (2009).
40. Phan, T. H. et al. EspH is a hypervirulence factor for *Mycobacterium marinum* and essential for the secretion of the ESX-1 substrates EspE and EspF. *PLoS Pathog.* **14**, e1007247 (2018).
41. Crosskey, T. D., Beckham, K. S. H. & Wilmanns, M. The ATPases of the mycobacterial type VII secretion system: structural and mechanistic insights into secretion. *Prog. Biophys. Mol. Biol.* **152**, 25–34 (2020).
42. Beckham, K. S. H. et al. Structure of the mycobacterial ESX-5 type VII secretion system hexameric pore complex. Preprint at <https://www.biorxiv.org/content/10.1101/2020.11.17.387225v1> (2020).
43. Bunduc, C. M. et al. Structure and dynamics of the ESX-5 type VII secretion system of *Mycobacterium tuberculosis*. Preprint at <https://www.biorxiv.org/content/10.1101/2020.12.02.408906v1> (2020).
44. Poweleit, N. et al. The structure of the endogenous ESX-3 secretion system. *eLife* **8**, e52983 (2019).
45. Hoffmann, C., Leis, A., Niederweis, M., Plietzko, J. M. & Engelhardt, H. Disclosure of the mycobacterial outer membrane: cryo-electron tomography and vitreous sections reveal the lipid bilayer structure. *Proc. Natl Acad. Sci. USA* **105**, 3963–3967 (2008).
46. Daffe, M. & Marrakchi, H. Unraveling the structure of the mycobacterial envelope. *Microbiol. Spectr.* <https://doi.org/10.1128/microbiolspec.GPP3-0027-2018> (2019).
47. Chiaradia, L. et al. Dissecting the mycobacterial cell envelope and defining the composition of the native mycomembrane. *Sci. Rep.* **7**, 12807 (2017).
48. Kalscheuer, R. et al. The *Mycobacterium tuberculosis* capsule: a cell structure with key implications in pathogenesis. *Biochem. J.* **476**, 1995–2016 (2019).
49. Renshaw, P. S. et al. Structure and function of the complex formed by the tuberculosis virulence factors CFP-10 and ESAT-6. *EMBO J.* **24**, 2491–2498 (2005).
50. Ates, L. S. et al. Essential role of the ESX-5 secretion system in outer membrane permeability of pathogenic mycobacteria. *PLoS Genet.* **11**, e1005190 (2015).
Ates et al. provide the first evidence that ESX-5 and PE–PPE proteins are involved in nutrient uptake across the outer membrane of slow-growing mycobacteria.
51. Abdallah, A. M. et al. The ESX-5 secretion system of *Mycobacterium marinum* modulates the macrophage response. *J. Immunol.* **181**, 7166–7175 (2008).
52. Gey van Pittius, N. C. et al. Evolution and expansion of the *Mycobacterium tuberculosis* PE and PPE multigene families and their association with the duplication of the ESAT-6 (esx) gene cluster regions. *BMC Evol. Biol.* **6**, 95 (2006).
53. Tufariello, J. M. et al. Separable roles for *Mycobacterium tuberculosis* ESX-3 effectors in iron acquisition and virulence. *Proc. Natl Acad. Sci. USA* **113**, E348–E357 (2016).
54. Serafini, A., Boldrin, F., Palu, G. & Manganello, R. Characterization of a *Mycobacterium tuberculosis* ESX-3 conditional mutant: essentiality and rescue by iron and zinc. *J. Bacteriol.* **191**, 6340–6344 (2009).
55. Siegrist, M. S. et al. Mycobacterial Esx-3 is required for mycobactin-mediated iron acquisition. *Proc. Natl Acad. Sci. USA* **106**, 18792–18797 (2009).
56. Mehra, A. et al. *Mycobacterium tuberculosis* type VII secreted effector EsxH targets host ESCRT to impair trafficking. *PLoS Pathog.* **9**, e1003734 (2013).
57. Portal-Celhay, C. et al. *Mycobacterium tuberculosis* EsxH inhibits ESCRT-dependent CD4⁺ T-cell activation. *Nat. Microbiol.* **2**, 16232 (2016).
58. Mittal, E. et al. *Mycobacterium tuberculosis* type VII secretion system effectors differentially impact the ESCRT endomembrane damage response. *mBio* **9**, e01765–18 (2018).
59. Simeone, R. et al. Phagosomal rupture by *Mycobacterium tuberculosis* results in toxicity and host cell death. *PLoS Pathog.* **8**, e1002507 (2012).
60. Augenstreich, J. et al. ESX-1 and phthiocerol dimycocerosates of *Mycobacterium tuberculosis* act in concert to cause phagosomal rupture and host cell apoptosis. *Cell. Microbiol.* **19**, e12726 (2017).
61. Houben, D. et al. ESX-1-mediated translocation to the cytosol controls virulence of mycobacteria. *Cell. Microbiol.* **14**, 1287–1298 (2012).
62. Beckwith, K. S. et al. Plasma membrane damage causes NLRP3 activation and pyroptosis during *Mycobacterium tuberculosis* infection. *Nat. Commun.* **11**, 2270 (2020).
63. Girard-Misguich, F. et al. [The most ancestral mycobacterial ESX-4 secretion system is essential for intracellular growth of *Mycobacterium abscessus* within environmental and human phagocytes]. *Med. Sci.* **34**, 795–797 (2018).
64. Laencina, L. et al. Identification of genes required for *Mycobacterium abscessus* growth in vivo with a prominent role of the ESX-4 locus. *Proc. Natl Acad. Sci. USA* **115**, E1002–E1011 (2018).
65. Gray, T. A. et al. Intercellular communication and conjugation are mediated by ESX secretion systems in mycobacteria. *Science* **354**, 347–350 (2016).
66. Bosserman, R. E. et al. WhiB6 regulation of ESX-1 gene expression is controlled by a negative feedback loop in *Mycobacterium marinum*. *Proc. Natl Acad. Sci. USA* **114**, E10772–E10781 (2017).
67. Sanchez, K. G. et al. EspM is a conserved transcription factor that regulates gene expression in response to the ESX-1 system. *mBio* **11**, e02807–e02819 (2020).
68. Kundu, M. The role of two-component systems in the physiology of *Mycobacterium tuberculosis*. *IUBMB Life* **70**, 710–717 (2018).
69. Broset, E., Martin, C. & Gonzalo-Asensio, J. Evolutionary landscape of the *Mycobacterium tuberculosis* complex from the viewpoint of PhoPR: implications for virulence regulation and application to vaccine development. *mBio* **6**, e01289–01215 (2015).
70. Frigui, W. et al. Control of *M. tuberculosis* ESAT-6 secretion and specific T cell recognition by PhoP. *PLoS Pathog.* **4**, e33 (2008).
71. Anil Kumar, V. et al. EspR-dependent ESAT-6 protein secretion of *Mycobacterium tuberculosis* requires the presence of virulence regulator PhoP. *J. Biol. Chem.* **291**, 19018–19030 (2016).
72. Fortune, S. M. et al. Mutually dependent secretion of proteins required for mycobacterial virulence. *Proc. Natl Acad. Sci. USA* **102**, 10676–10681 (2005).

73. MacGurn, J. A., Raghavan, S., Stanley, S. A. & Cox, J. S. A non-RD1 gene cluster is required for Snm secretion in *Mycobacterium tuberculosis*. *Mol. Microbiol.* **57**, 1653–1663 (2005).
74. Pang, X. et al. MprAB regulates the espA operon in *Mycobacterium tuberculosis* and modulates ESX-1 function and host cytokine response. *J. Bacteriol.* **195**, 66–75 (2013).
75. Kahramanoglu, C. et al. Genomic mapping of cAMP receptor protein (CRP Mt) in *Mycobacterium tuberculosis*: relation to transcriptional start sites and the role of CRP Mt as a transcription factor. *Nucleic Acids Res.* **42**, 8320–8329 (2014).
76. Gordon, B. R. et al. Lsr2 is a nucleoid-associated protein that targets AT-rich sequences and virulence genes in *Mycobacterium tuberculosis*. *Proc. Natl Acad. Sci. USA* **107**, 5154–5159 (2010).
77. Blasco, B. et al. Virulence regulator EspR of *Mycobacterium tuberculosis* is a nucleoid-associated protein. *PLoS Pathog.* **8**, e1002621 (2012).
78. Rosenberg, O. S. et al. EspR, a key regulator of *Mycobacterium tuberculosis* virulence, adopts a unique dimeric structure among helix-turn-helix proteins. *Proc. Natl Acad. Sci. USA* **108**, 13450–13455 (2011).
79. Gonzalo-Asensio, J. et al. Evolutionary history of tuberculosis shaped by conserved mutations in the PhoPR virulence regulator. *Proc. Natl Acad. Sci. USA* **111**, 11491–11496 (2014).
80. Ates, L. S. et al. Unexpected genomic and phenotypic diversity of *Mycobacterium africanum* lineage 5 affects drug resistance, protein secretion, and immunogenicity. *Genome Biol. Evol.* **10**, 1858–1874 (2018).
81. Abdallah, A. M. et al. Integrated transcriptomic and proteomic analysis of pathogenic mycobacteria and their *esx-1* mutants reveal secretion-dependent regulation of ESX-1 substrates and WhiB6 as a transcriptional regulator. *PLoS ONE* **14**, e0211003 (2019).
82. Solans, L. et al. A specific polymorphism in *Mycobacterium tuberculosis* H37Rv causes differential ESAT-6 expression and identifies WhiB6 as a novel ESX-1 component. *Infect. Immun.* **82**, 3446–3456 (2014).
83. Serafini, A., Pisu, D., Palu, G., Rodriguez, G. M. & Manganello, R. The ESX-3 secretion system is necessary for iron and zinc homeostasis in *Mycobacterium tuberculosis*. *PLoS ONE* **8**, e78351 (2013).
84. Maciag, A., Piazza, A., Riccardi, G. & Milano, A. Transcriptional analysis of ESAT-6 cluster 3 in *Mycobacterium smegmatis*. *BMC Microbiol.* **9**, 48 (2009).
85. Rodriguez, G. M., Voskuil, M. I., Gold, B., Schoolnik, G. K. & Smith, I. IdeR, an essential gene in *Mycobacterium tuberculosis*: role of IdeR in iron-dependent gene expression, iron metabolism, and oxidative stress response. *Infect. Immun.* **70**, 3371–3381 (2002).
86. Elliott, S. R. & Tischler, A. D. Phosphate starvation: a novel signal that triggers ESX-5 secretion in *Mycobacterium tuberculosis*. *Mol. Microbiol.* **100**, 510–526 (2016).
87. Beckham, K. S. et al. Structure of the mycobacterial ESX-5 type VII secretion system membrane complex by single-particle analysis. *Nat. Microbiol.* **2**, 17047 (2017).
Beckham et al. present the first negative-stain structure of the ESX-5 core complex hexamer (EccB–EccE) and provide evidence for the hexameric organization of T7SS core complexes.
88. Wagner, J. M. et al. Structures of EccB1 and EccD1 from the core complex of the mycobacterial ESX-1 type VII secretion system. *BMC Struct. Biol.* **16**, 5 (2016).
89. Zhang, X. L. et al. Core component EccB1 of the *Mycobacterium tuberculosis* type VII secretion system is a periplasmic ATPase. *FASEB J.* **29**, 4804–4814 (2015).
90. Rosenberg, O. S. et al. Substrates control multimerization and activation of the multi-domain ATPase motor of type VII secretion. *Cell* **161**, 501–512 (2015).
This study shows the first co-structure of the substrate recognition domain with a signal peptide, and shows that oligomerization and allosteric activation are required for activation of the T7SS.
91. Iyer, L. M., Makarova, K. S., Koonin, E. V. & Aravind, L. Comparative genomics of the FtsK-HerA superfamily of pumping ATPases: implications for the origins of chromosome segregation, cell division and viral capsid packaging. *Nucleic Acids Res.* **32**, 5260–5279 (2004).
92. Puchades, C., Sandate, C. R. & Lander, G. C. The molecular principles governing the activity and functional diversity of AAA+ proteins. *Nat. Rev. Mol. Cell Biol.* **21**, 43–58 (2020).
93. Wang, S. et al. Structural insights into substrate recognition by the type VII secretion system. *Protein Cell* **11**, 124–137 (2020).
94. Zoltner, M. et al. EssC: domain structures inform on the elusive translocation channel in the type VII secretion system. *Biochem. J.* **473**, 1941–1952 (2016).
95. Klein, T. A., Ahmad, S. & Whitney, J. C. Contact-dependent interbacterial antagonism mediated by protein secretion machines. *Trends Microbiol.* **28**, 387–400 (2020).
96. Taylor, J. C. et al. A type VII secretion system of *Streptococcus gallolyticus* subsp. *gallolyticus* contributes to gut colonization and the development of colon tumors. *PLoS Pathog.* **17**, e1009182 (2021).
97. Ulhuq, F. R. et al. A membrane-depolarizing toxin substrate of the *Staphylococcus aureus* type VII secretion system mediates intraspecies competition. *Proc. Natl Acad. Sci. USA* **117**, 20836–20847 (2020).
98. Tassinari, M. et al. Central role and structure of the membrane pseudokinase YrkC in the antibacterial *Bacillus subtilis* type VII secretion system. Preprint at <https://www.biorxiv.org/content/10.1101/2020.05.09.085852v1> (2020).
99. Whitney, J. C. et al. A broadly distributed toxin family mediates contact-dependent antagonism between gram-positive bacteria. *eLife* **6**, e26938 (2017).
100. Cao, Z., Casabona, M. G., Kneuper, H., Chalmers, J. D. & Palmer, T. The type VII secretion system of *Staphylococcus aureus* secretes a nuclease toxin that targets competitor bacteria. *Nat. Microbiol.* **2**, 16183 (2016).
101. Burts, M. L., Williams, W. A., DeBord, K. & Missiakas, D. M. EsxA and EsxB are secreted by an ESAT-6-like system that is required for the pathogenesis of *Staphylococcus aureus* infections. *Proc. Natl Acad. Sci. USA* **102**, 1169–1174 (2005).
102. Anderson, M., Aly, K. A., Chen, Y. H. & Missiakas, D. Secretion of atypical protein substrates by the ESAT-6 secretion system of *Staphylococcus aureus*. *Mol. Microbiol.* **90**, 734–743 (2013).
103. Kneuper, H. et al. Heterogeneity in *ess* transcriptional organization and variable contribution of the Ess/Type VII protein secretion system to virulence across closely related *Staphylococcus aureus* strains. *Mol. Microbiol.* **93**, 928–943 (2014).
104. Casabona, M. G. et al. Functional analysis of the EsaB component of the *Staphylococcus aureus* Type VII secretion system. *Microbiology* <https://doi.org/10.1099/mic.0.000580> (2017).
105. Warne, B. et al. The Ess/Type VII secretion system of *Staphylococcus aureus* shows unexpected genetic diversity. *BMC Genomics* **17**, 222 (2016).
106. Lebeurre, J. et al. Comparative genome analysis of *Staphylococcus lugdunensis* shows clonal complex-dependent diversity of the putative virulence factor, *ess/type VII* locus. *Front. Microbiol.* **10**, 2479 (2019).
107. Zoltner, M., Fyfe, P. K., Palmer, T. & Hunter, W. N. Characterization of *Staphylococcus aureus* EssB, an integral membrane component of the Type VII secretion system: atomic resolution crystal structure of the cytoplasmic segment. *Biochem. J.* **449**, 469–477 (2013).
108. Zoltner, M. et al. The architecture of EssB, an integral membrane component of the type VII secretion system. *Structure* **21**, 595–603 (2013).
109. Klein, T. A. et al. Structure of the extracellular region of the bacterial type VII secretion system subunit EsaA. *Structure* **29**, 177–185 e176 (2021).
110. van den Ent, F. & Lowe, J. Crystal structure of the ubiquitin-like protein YrkD from *Bacillus subtilis*. *FEBS Lett.* **579**, 3837–3841 (2005).
111. Tanaka, Y. et al. Crystal structure analysis reveals a novel forkhead-associated domain of ESAT-6 secretion system C protein in *Staphylococcus aureus*. *Proteins* **69**, 659–664 (2007).
112. Mietrach, N., Damian-Aparicio, D., Mielich-Suss, B., Lopez, D. & Geibel, S. Substrate interaction with the EssC coupling protein of the type VII secretion system. *J. Bacteriol.* **202**, e00646–19 (2020).
113. Jager, F., Zoltner, M., Kneuper, H., Hunter, W. N. & Palmer, T. Membrane interactions and self-association of components of the Ess/Type VII secretion system of *Staphylococcus aureus*. *FEBS Lett.* **590**, 349–357 (2016).
114. Jager, F., Kneuper, H. & Palmer, T. EssC is a specificity determinant for *Staphylococcus aureus* type VII secretion. *Microbiology* **164**, 816–820 (2018).
115. Dreisbach, A. et al. Profiling the surfacome of *Staphylococcus aureus*. *Proteomics* **10**, 3082–3096 (2010).
116. Mietrach, N. et al. The conserved core component EsaA mediates bacterial killing by the type VII secretion system. *Res. Square* <https://doi.org/10.21203/rs.3.rs-95626/v1> (2020).
117. Bunduc, C. M., Ummels, R., Bitter, W. & Houben, E. N. G. Species-specific secretion of ESX-5 type VII substrates is determined by the linker 2 of EccC5. *Mol. Microbiol.* **114**, 66–76 (2020).
118. de Jonge, M. I. et al. ESAT-6 from *Mycobacterium tuberculosis* dissociates from its putative chaperone CFP-10 under acidic conditions and exhibits membrane-lysing activity. *J. Bacteriol.* **189**, 6028–6034 (2007).
119. Okkels, L. M. et al. CFP10 discriminates between nonacetylated and acetylated ESAT-6 of *Mycobacterium tuberculosis* by differential interaction. *Proteomics* **4**, 2954–2960 (2004).
120. Brown, G. D. et al. The mycosins of *Mycobacterium tuberculosis* H37Rv: a family of subtilisin-like serine proteases. *Gene* **254**, 147–155 (2000).
121. Dave, J. A., Gey van Pittius, N. C., Beyers, A. D., Ehlers, M. R. & Brown, G. D. Mycosin-1, a subtilisin-like serine protease of *Mycobacterium tuberculosis*, is cell wall-associated and expressed during infection of macrophages. *BMC Microbiol.* **2**, 30 (2002).
122. McLaughlin, B. et al. A mycobacterial ESX-1-secreted virulence factor with unique requirements for export. *PLoS Pathog.* **3**, e105 (2007).
123. Xu, J. et al. A unique Mycobacterium ESX-1 protein co-secretes with CFP-10/ESAT-6 and is necessary for inhibiting phagosome maturation. *Mol. Microbiol.* **66**, 787–800 (2007).
124. van Winden, V. J. et al. Mycosins are required for the stabilization of the ESX-1 and ESX-5 type VII secretion membrane complexes. *mBio* **7**, e01471–16 (2016).
125. Ekiert, D. C. & Cox, J. S. Structure of a PE-PPE-EspG complex from *Mycobacterium tuberculosis* reveals molecular specificity of ESX protein secretion. *Proc. Natl Acad. Sci. USA* **111**, 14758–14763 (2014).
This study presents the first structure of a PE–PPE substrate heterodimer bound to the chaperone EspG and shows that PE–PPE substrates interact specifically with their cognate chaperones.
126. Korotkova, N. et al. Structure of the Mycobacterium tuberculosis type VII secretion system chaperone EspG5 in complex with PE25-PPE41 dimer. *Mol. Microbiol.* **94**, 367–382 (2014).
127. Phan, T. H., Ummels, R., Bitter, W. & Houben, E. N. Identification of a substrate domain that determines system specificity in mycobacterial type VII secretion systems. *Sci. Rep.* **7**, 42704 (2017).
Together with the study of Ekiert and Cox (2014), this study establishes that EspG determines the system specificity of PE–PPE substrates.
128. Damen, M. P. M. et al. Modification of a PE/PPE substrate pair reroutes an Esx substrate pair from the mycobacterial ESX-1 type VII secretion system to the ESX-5 system. *J. Biol. Chem.* **295**, 5960–5969 (2020).
129. Williamson, Z. A., Chaton, C. T., Ciocca, W. A., Korotkova, N. & Korotkov, K. V. PES-PPE4-EspG3 heterotrimer structure from mycobacterial ESX-3 secretion system gives insight into cognate substrate recognition by ESX systems. *J. Biol. Chem.* **295**, 12706–12715 (2020).
130. Wagner, J. M., Evans, T. J. & Korotkov, K. V. Crystal structure of the N-terminal domain of EccA(1) ATPase from the ESX-1 secretion system of *Mycobacterium tuberculosis*. *Proteins* **82**, 159–163 (2014).
131. Wang, Q. et al. PE/PPE proteins mediate nutrient transport across the outer membrane of *Mycobacterium tuberculosis*. *Science* **367**, 1147–1151 (2020).
Wang et al. provide the first detailed study of porins formed by PE–PPE proteins in the mycobacterial cell envelope.
132. Lou, Y., Rybniker, J., Sala, C. & Cole, S. T. EspC forms a filamentous structure in the cell envelope of *Mycobacterium tuberculosis* and impacts ESX-1 secretion. *Mol. Microbiol.* **103**, 26–38 (2017).
133. Solomonson, M. et al. Structure of EspB from the ESX-1 type VII secretion system and insights into its export mechanism. *Structure* **23**, 571–583 (2015).

134. Gijbsers, A. et al. Priming mycobacterial ESX-secreted protein B to form a channel-like structure. Preprint at <https://www.biorxiv.org/content/10.1101/2021.01.02.425093v1.full> (2021).
135. Piton, J., Pojer, F., Wakatsuki, S., Gati, C. & Cole, S. T. High resolution CryoEM structure of the ring-shaped virulence factor EspB from *Mycobacterium tuberculosis*. *J. Struct. Biol.* **4**, 100029 (2020).
136. Chen, J. M. et al. *Mycobacterium tuberculosis* EspB binds phospholipids and mediates ESxA-independent virulence. *Mol. Microbiol.* **89**, 1154–1166 (2013).
137. Punjani, A. & Fleet, D. J. 3D variability analysis: resolving continuous flexibility and discrete heterogeneity from single particle cryo-EM images. *J. Struct. Biol.* **213**, 107702 (2021).
138. Punjani, A., Rubinstein, J. L., Fleet, D. J. & Brubaker, M. A. cryoSPARC: algorithms for rapid unsupervised cryo-EM structure determination. *Nat. Methods* **14**, 290–296 (2017).
139. Groschel, M. I., Sayes, F., Simeone, R., Majlessi, L. & Brosch, R. ESX secretion systems: mycobacterial evolution to counter host immunity. *Nat. Rev. Microbiol.* **14**, 677–691 (2016).
140. Khan, H. S. et al. Identification of scavenger receptor B1 as the airway microfold cell receptor for *Mycobacterium tuberculosis*. *eLife* **9**, e52551 (2020).
141. Stamm, L. M. et al. *Mycobacterium marinum* escapes from phagosomes and is propelled by actin-based motility. *J. Exp. Med.* **198**, 1361–1368 (2003).
142. van der Wel, N. et al. *M. tuberculosis* and *M. leprae* translocate from the phagolysosome to the cytosol in myeloid cells. *Cell* **129**, 1287–1298 (2007).
143. Simeone, R. et al. Cytosolic access of *Mycobacterium tuberculosis*: critical impact of phagosomal acidification control and demonstration of occurrence in vivo. *PLoS Pathog.* **11**, e1004650 (2015).
144. Conrad, W. H. et al. Mycobacterial ESX-1 secretion system mediates host cell lysis through bacterium contact-dependent gross membrane disruptions. *Proc. Natl Acad. Sci. USA* **114**, 1371–1376 (2017).
145. Liénard, J. et al. The *Mycobacterium marinum* ESX-1 system mediates phagosomal permeabilization and type I interferon production via separable mechanisms. *Proc. Natl Acad. Sci. USA* **117**, 1160–1166 (2020).
146. Quigley, J. et al. The cell wall lipid PDIM contributes to phagosomal escape and host cell exit of *Mycobacterium tuberculosis*. *mBio* **8**, e00148–17 (2017).
147. Skowyrza, M. L., Schlesinger, P. H., Naismith, T. V. & Hanson, P. I. Triggered recruitment of ESCRT machinery promotes endolysosomal repair. *Science* **360**, eaar5078 (2018).
148. Stanley, S. A., Johndrow, J. E., Manzanillo, P. & Cox, J. S. The type I IFN response to infection with *Mycobacterium tuberculosis* requires ESX-1-mediated secretion and contributes to pathogenesis. *J. Immunol.* **178**, 3143–3152 (2007).
149. Collins, A. C. et al. Cyclic GMP-AMP synthase is an innate immune DNA sensor for *Mycobacterium tuberculosis*. *Cell Host Microbe* **17**, 820–828 (2015).
150. Watson, R. O., Manzanillo, P. S. & Cox, J. S. Extracellular *M. tuberculosis* DNA targets bacteria for autophagy by activating the host DNA-sensing pathway. *Cell* **150**, 803–815 (2012).
151. Wassermann, R. et al. *Mycobacterium tuberculosis* differentially activates cGAS- and inflammasome-dependent intracellular immune responses through ESX-1. *Cell Host Microbe* **17**, 799–810 (2015).
152. Aguilo, J. I. et al. ESX-1-induced apoptosis is involved in cell-to-cell spread of *Mycobacterium tuberculosis*. *Cell. Microbiol.* **15**, 1994–2005 (2013).
153. Volkman, H. E. et al. Tuberculous granuloma induction via interaction of a bacterial secreted protein with host epithelium. *Science* **327**, 466–469 (2010).
154. Kapoor, N. et al. Human granuloma in vitro model, for TB dormancy and resuscitation. *PLoS ONE* **8**, e53657 (2013).
155. Davis, J. M. & Ramakrishnan, L. The role of the granuloma in expansion and dissemination of early tuberculous infection. *Cell* **136**, 37–49 (2009).
156. Stoop, E. J. et al. Zebrafish embryo screen for mycobacterial genes involved in the initiation of granuloma formation reveals a newly identified ESX-1 component. *Dis. Model. Mech.* **4**, 526–536 (2011).
157. Zhang, L. et al. Comprehensive analysis of iron utilization by *Mycobacterium tuberculosis*. *PLoS Pathog.* **16**, e1008337 (2020).
158. Chao, A., Sieminski, P. J., Owens, C. P. & Goulding, C. W. Iron acquisition in *Mycobacterium tuberculosis*. *Chem. Rev.* **119**, 1193–1220 (2019).
159. Santucci, P. et al. Dissecting the membrane lipid binding properties and lipase activity of *Mycobacterium tuberculosis* LipY domains. *FEBS J.* **286**, 3164–3181 (2019).
160. Boritsch, E. C. et al. Key experimental evidence of chromosomal DNA transfer among selected tuberculosis-causing mycobacteria. *Proc. Natl Acad. Sci. USA* **113**, 9876–9881 (2016).
161. Flint, J. L., Kowalski, J. C., Karnati, P. K. & Derbyshire, K. M. The RD1 virulence locus of *Mycobacterium tuberculosis* regulates DNA transfer in *Mycobacterium smegmatis*. *Proc. Natl Acad. Sci. USA* **101**, 12598–12603 (2004).
162. Gray, T. A., Krywy, J. A., Harold, J., Palumbo, M. J. & Derbyshire, K. M. Distributive conjugal transfer in mycobacteria generates progeny with meiotic-like genome-wide mosaicism, allowing mapping of a mating identity locus. *PLoS Biol.* **11**, e1001602 (2013).
163. Clark, R. R. et al. Direct cell-cell contact activates SigM to express the ESX-4 secretion system in *Mycobacterium smegmatis*. *Proc. Natl Acad. Sci. USA* **115**, E6595–E6603 (2018).
164. Coros, A., Callahan, B., Battaglioli, E. & Derbyshire, K. M. The specialized secretory apparatus ESX-1 is essential for DNA transfer in *Mycobacterium smegmatis*. *Mol. Microbiol.* **69**, 794–808 (2008).
165. Gray, T. A. & Derbyshire, K. M. Blending genomes: distributive conjugal transfer in mycobacteria, a sexier form of HGT. *Mol. Microbiol.* **108**, 601–613 (2018).
166. van Winden, V. J. C., Damen, M. P. M., Ummels, R., Bitter, W. & Houben, E. N. G. Protease domain and transmembrane domain of the type VII secretion mycosin protease determine system-specific functioning in mycobacteria. *J. Biol. Chem.* **294**, 4806–4814 (2019).
167. Sani, M. et al. Direct visualization by cryo-EM of the mycobacterial capsular layer: a labile structure containing ESX-1-secreted proteins. *PLoS Pathog.* **6**, e1000794 (2010).
168. Garces, A. et al. EspA acts as a critical mediator of ESX1-dependent virulence in *Mycobacterium tuberculosis* by affecting bacterial cell wall integrity. *PLoS Pathog.* **6**, e1000957 (2010).
169. Ates, L. S. et al. The ESX-5 system of pathogenic mycobacteria is involved in capsule integrity and virulence through its substrate PPE10. *PLoS Pathog.* **12**, e1005696 (2016).
170. Akpe San Roman, S. et al. A heterodimer of EsxA and EsxB is involved in sporulation and is secreted by a type VII secretion system in *Streptomyces coelicolor*. *Microbiology* **156**, 1719–1729 (2010).
171. Chatterjee, A., Willett, J. L. E., Dunny, G. M. & Duerkop, B. A. Phage infection and sub-lethal antibiotic exposure mediate *Enterococcus faecalis* type VII secretion system dependent inhibition of bystander bacteria. *PLoS Genet.* **17**, e1009204 (2021).
172. Chatterjee, A. et al. Parallel genomics uncover novel enterococcal-bacteriophage interactions. *mBio* <https://doi.org/10.1128/mBio.03120-19> (2020).
173. Lopez, M. S. et al. Host-derived fatty acids activate type VII secretion in *Staphylococcus aureus*. *Proc. Natl Acad. Sci. USA* **114**, 11223–11228 (2017).
174. Psonis, J. J. & Thanassi, D. G. Therapeutic approaches targeting the assembly and function of chaperoneusher Pili. *EcoSal Plus* <https://doi.org/10.1128/ecosalplus.ESP-0033-2018> (2019).
175. Fasciano, A. C., Shaban, L. & Mecsas, J. Promises and challenges of the type three secretion system injectisome as an antivirulence target. *EcoSal Plus* <https://doi.org/10.1128/ecosalplus.ESP-0032-2018> (2019).
176. Bitter, W. & Kuijl, C. Targeting bacterial virulence: the coming out of type VII secretion inhibitors. *Cell Host Microbe* **16**, 430–432 (2014).
177. Rybniker, J. et al. Anticytolytic screen identifies inhibitors of mycobacterial virulence protein secretion. *Cell Host Microbe* **16**, 538–548 (2014).
178. Massey, T. H., Mercogliano, C. P., Yates, J., Sherratt, D. J. & Löwe, J. Double-stranded DNA translocation: structure and mechanism of hexameric FtsK. *Mol. Cell* **23**, 457–469 (2006).
179. Daleke, M. H. et al. General secretion signal for the mycobacterial type VII secretion pathway. *Proc. Natl Acad. Sci. USA* **109**, 11342–11347 (2012). **This study identifies the amino acid sequence YXXXD/E as a general type VII secretion signal.**
180. Poulsen, C., Panjikar, S., Holton, S. J., Wilmanns, M. & Song, Y. H. W.XG100 protein superfamily consists of three subfamilies and exhibits an alpha-helical C-terminal conserved residue pattern. *PLoS ONE* **9**, e89313 (2014).
181. Syssoeva, T. A., Zepeda-Rivera, M. A., Huppert, L. A. & Burton, B. M. Dimer recognition and secretion by the ESX secretion system in *Bacillus subtilis*. *Proc. Natl Acad. Sci. USA* **111**, 7653–7658 (2014).
182. Korotkova, N. et al. Structure of EspB, a secreted substrate of the ESX-1 secretion system of *Mycobacterium tuberculosis*. *J. Struct. Biol.* **191**, 236–244 (2015).
183. Pallen, M. J. The ESAT-6/WXG100 superfamily – and a new Gram-positive secretion system? *Trends Microbiol.* **10**, 209–212 (2002).
184. Champion, P. A., Stanley, S. A., Champion, M. M., Brown, E. J. & Cox, J. S. C-terminal signal sequence promotes virulence factor secretion in *Mycobacterium tuberculosis*. *Science* **313**, 1632–1636 (2006). **This study shows that the C terminus of WXG100 contains a signal peptide crucial for the interactions of these proteins with the C-terminal segment of the EssC coupling protein.**
185. Ates, L. S. New insights into the mycobacterial PE and PPE proteins provide a framework for future research. *Mol. Microbiol.* **113**, 4–21 (2020).
186. Meng, L. et al. PPE38 protein of mycobacterium tuberculosis inhibits macrophage MHC class I expression and dampens CD8(+) T cell responses. *Front. Cell Infect. Microbiol.* **7**, 68 (2017).
187. Brennan, M. J. The enigmatic PE/PPE multigene family of mycobacteria and tuberculosis vaccination. *Infect. Immun.* **85**, e00969–16 (2017).

Acknowledgements

This work was funded by the Elite Network of Bavaria (N-BM-2013-246 to S.G.), bayresg.net (S.G.), grant SAF2017-82632-P to O.L. from the Spanish Ministry of Science, Innovation and Universities (MCIU/AEI), co-funded by the European Regional Development Fund, the support of the Spanish National Institute of Health Carlos III provided to CNIO, and grants Y2018/BI04747 and P2018/NMT4443 from the Autonomous Region of Madrid and co-funded by the European Social Fund and the European Regional Development Fund to the activities of the group directed by O.L.

Author contributions

A.R.-C. and S.G. researched data for the article. A.R.-C., N.F. and S.G. contributed substantially to discussion of the content. A.R.-C., O.L. and S.G. wrote the article. All authors reviewed and/or edited the manuscript before submission.

Competing interests

The authors declare no competing interests.

Peer review information

Nature Reviews Microbiology thanks J. Cox and the other, anonymous, reviewer(s) for their contribution to the peer review of this work.

Publisher's note

Springer Nature remains neutral with regard to jurisdictional claims in published maps and institutional affiliations.

Supplementary information

The online version contains supplementary material available at <https://doi.org/10.1038/s41579-021-00560-5>.

© Springer Nature Limited 2021